MARTIN MARIETTA ENERGY SYSTEMS LIBRARIES

3 4456 0279947 0

(LACE TR-023)
ORNL/M-352

ornl

OAK RIDGE
NATIONAL
LABORATORY

MARTIN MARIETTA

Summary of Pretest Aerosol Code Results for LWR Aerosol Containment Experiment (LACE) LA3

A. L. Wright
P. C. Arwood

OAK RIDGE NATIONAL LABORATORY
CENTRAL RESEARCH LIBRARY
CIRCULATION SECTION
4500N ROOM 175
LIBRARY LOAN COPY
DO NOT TRANSFER TO ANOTHER PERSON
If you wish someone else to see this report, send in name with report and the library will arrange a loan.

OPERATED BY
MARTIN MARIETTA ENERGY SYSTEMS, INC.
FOR THE UNITED STATES
DEPARTMENT OF ENERGY

This report was prepared as an account of work sponsored by an agency of the United States Government. Neither the United States Government nor any agency thereof, nor any of their employees, makes any warranty, express or implied, or assumes any legal liability or responsibility for the accuracy, completeness, or usefulness of any information, apparatus, product, or process disclosed, or represents that its use would not infringe privately owned rights. Reference herein to any specific commercial product, process, or service by trade name, trademark, manufacturer, or otherwise, does not necessarily constitute or imply its endorsement, recommendation, or favoring by the United States Government or any agency thereof. The views and opinions of authors expressed herein do not necessarily state or reflect those of the United States Government or any agency thereof.

LACE TR-023
ORNL/M-352

Chemical Technology Division

SUMMARY OF PRETEST AEROSOL CODE RESULTS FOR LWR AEROSOL CONTAINMENT EXPERIMENT (LACE) LA3

Principal Investigators

A. L. Wright
P. C. Arwood

Prepared for
ELECTRIC POWER RESEARCH INSTITUTE
3412 Hillview Avenue
Palo Alto, California 94303

EPRI Project No. 2135-18

Date Issued: November 1987

Prepared by the
OAK RIDGE NATIONAL LABORATORY
Oak Ridge, Tennessee 37831
operated by
MARTIN MARIETTA ENERGY SYSTEMS, INC.
for the
U.S. DEPARTMENT OF ENERGY
under contract DE-AC05-840R21400

MARTIN MARIETTA ENERGY SYSTEMS LIBRARIES

3 4456 0279947 0

[redacted]

NOTICE

This report was prepared by the organization(s) named below as an account of work sponsored by the Electric Power Research Institute, Inc. (EPRI). Neither EPRI, members of EPRI, the organization(s) named below, nor any person acting on behalf of any of them: (a) makes any warranty, express or implied, with respect to the use of any information, apparatus, method, or process disclosed in this report or that such use may not infringe privately owned rights; or (b) assumes any liabilities with respect to the use of, or for damages resulting from the use of, any information, apparatus, method or process disclosed in this report.

Prepared by

OAK RIDGE NATIONAL LABORATORY
Oak Ridge, Tennessee

[illegible]

CONTENTS

		Page
ABSTRACT		vii
1.	INTRODUCTION	1
2.	SUMMARY OF CODE INPUTS AND REQUESTED CODE OUTPUTS FOR LA3 PRETEST CALCULATIONS	2
3.	COMPARATIVE CALCULATIONS OF TURBULENT-DEPOSITION VELOCITIES FOR LA1 AND LA3 TEST CONDITIONS	6
4.	RESULTS FROM INITIAL LA3 PRETEST CALCULATIONS	18
5.	RESULTS FROM LA3B BENCHMARK CALCULATIONS	36
6.	SUMMARY AND CONCLUSIONS	43
7.	ACKNOWLEDGMENTS	45
8.	REFERENCES	45

ABSTRACT

This report describes work performed as part of the LACE Code-Experiment Comparison Project, which is sponsored by the Electric Power Research Institute (EPRI Project No. 2135-18). The LACE tests are being performed at the Westinghouse Hanford Engineering Development Laboratory. LACE test LA3 consisted of three experiments (LA3A, LA3B, and LA3C) designed to simulate aerosol flow through a pipe for "containment bypass" accident sequence conditions. The report presents and summarizes comparisons of results from pretest calculations performed to model LACE test LA3. Two sets of calculations are discussed: (1) calculations to model LA3A, LA3B, and LA3C and (2) a benchmark calculation to model LA3B. In the benchmark calculation, all code users were to have used exactly the same code inputs.

SUMMARY OF PRETEST AEROSOL CODE RESULTS FOR LWR AEROSOL CONTAINMENT EXPERIMENT (LACE) LA3

A. L. Wright
P. C. Arwood

1. INTRODUCTION

The Light-Water Reactor (LWR) Aerosol Containment Experiments (LACE) are being performed to investigate experimentally, on a large scale, the aerosol retention behavior in containment and associated piping under simulated severe LWR accident conditions. An additional, and equally important, objective of these tests is to provide a data base for validating aerosol containment computer codes and related thermal-hydraulic computer codes. The LACE tests are internationally funded and are being performed at the Westinghouse Hanford Engineering Development Laboratory (HEDL) under the leadership of an overall project board and the Electric Power Research Institute (EPRI).

The overall LACE project has two components: (1) the experiments being performed at HEDL and (2) aerosol-transport and thermal-hydraulic code-comparison activities. The aerosol-transport code-comparison activities are being coordinated at Oak Ridge National Laboratory (ORNL), Oak Ridge, Tennessee, while the thermal-hydraulic code-comparison activities are being coordinated at Intermountain Technologies, Inc. (ITI), Idaho Falls, Idaho.

For each of the six planned LACE tests, pretest and blind posttest aerosol code calculations are being performed. The ORNL code-comparison activities include (1) providing guidance to participating aerosol code analysts to help them in performing calculations, (2) compiling the results from calculations, and (3) critically evaluating the code results and comparisons with the test data.

This report summarizes the results from pretest calculations performed for the LA3 test series. The LA3 experiments, designated as LA3A, LA3B, and LA3C, were designed to investigate aerosol behavior

during flow through a 0.063-m-diam, 28.8-m-long test pipe for simulated "containment bypass" accident sequence conditions. The next section of this report summarizes the defined code inputs and requested code outputs for the LA3 pretest calculations. For the LA3 test conditions, turbulent deposition is the major deposition mechanism. Section 3 presents calculations of deposition velocities vs particle size for LA3 and LA1 test conditions, using the turbulent-deposition models employed in the codes. Sections 4 and 5 present the results of the pretest calculations. Calculations were first performed for the entire LA3 series; a code benchmark calculation for the LA3B test was also performed. Finally, a summary of the results and insights gained from the LA3 pretest calculations is presented in Sect. 6.

2. SUMMARY OF CODE INPUTS AND REQUESTED CODE OUTPUTS FOR LA3 PRETEST CALCULATIONS

On the basis of information in the project test plan,[1] a guidance letter defining conditions for LA3 pretest calculations was sent to LACE participants.[2] Tables 1 to 3 present the information used by the code analysts to perform the initial series of LA3 pretest calculations. As noted in Table 1, pipe sections 4 through 21 were modeled in the calculations. As noted in Table 2, the major variables in the LA3 test series were the flow velocity through the test pipe and the MnO/CsOH aerosol mass ratio. Aerosol source size-distribution data are defined in Table 3.

Table 4 summarizes the requested LA3 code output parameters. As we did for LA1 posttest calculations, we requested that code users provide aerosol deposition and size data for each of the "control volumes" that was used in their calculations. We also requested that the code users provide deposition information for each mechanism (turbulent deposition, settling, thermophoresis, etc.) that was important in their calculations.

As will be discussed in detail in Sect. 4, different users of the TRAP-MELT2 code obtained different results from their calculations. To investigate why this may have occurred, a benchmark calculation was performed for LA3B test conditions. In this calculation, all investigators

Table 1. LA3 test pipe geometry[a]

Section No.	Pipe description	Flow direction	Diameter (cm)	Length (m)
1a	Straight	East	30	1.52
1b	90° bend		30	0.72
1c	Reducer	Up	30–10	0.28
2	Ball valve	Up	10	0.23
3	Reducer	Up	10–6.3	0.28
4	Straight	Up	6.3	2.26
5	90° bend[b]		6.3	0.38
6	Ball valve	West	6.3	0.19
7	Straight	West	6.3	4.20
8	90° bend[b]		6.3	0.38
9	Straight	South	6.3	2.58
10	Straight	South	6.3	4.32
11	90° bend[b]		6.3	0.38
12	Straight	East	6.3	4.32
13	Straight	East	6.3	3.10
14	90° bend[b]		6.3	0.55
15	Straight	North	6.3	1.65
16	Ball valve	North	6.3	0.19
17	90° bend[b]		6.3	0.55
18	Straight	Down	6.3	2.14
19	90° bend[b]		6.3	0.38
20	Ball valve	West	6.3	0.19
21	Straight	West	6.3	1.09
22	Transition	West	6.3–30	1.17
23a	Straight	West	30	1.95
23b	90° bend[b]	Up	30	0.58

[a]For LA3 pretest calculations, ONLY sections 4 through 21 were modeled; the overall length of sections 4 through 21 is 28.85 m.

[b]Radius of pipe bends in 6.3-cm-diam pipe is 9.5 cm.

Table 2. Summary of information needed for LA3 pretest calculations[a]

	LA3A	LA3B	LA3C
Test pipe gas flow rates (g/s)			
Steam	62.5	12.5	12.5
Nitrogen	91.7	18.3	18.3
Helium	0.6	0.3	0.3
Argon	1.4	0.7	0.7
Volumetric steam fraction[b]	0.5	0.5	0.5
Gas mixture viscosity (g/cm-s)	0.00024	0.00024	0.00024
Pressure (kPa absolute)			
Test pipe inlet[b]	174	109	109
Test pipe outlet[b]	123	107	107
Gas temperature (°C)			
Test pipe inlet[b]	300	300	300
Test pipe outlet[b]	275	200	200
Wall temperature (°C)			
Test pipe inlet[b]	295	285	285
Test pipe outlet[b]	270	185	185
Gas velocity (m/s)			
Test pipe inlet[b]	61	20	20
Test pipe outlet[b]	87	20	20
Aerosol source to test pipe (g/s)			
CsOH source rate	0.12	0.12	0.5
MnO source rate	1.0	1.0	1.0
Aerosol source size parameters			
Aerodynamic mass-median diameter (μm)[b]	2.0	2.0	2.0
Geometric standard deviation[b]	2.0	2.0	2.0
Aerosol shape factors	1.0	1.0	1.0
Aerosol source duration (min)	60	60	60

[a]Data from LA3 test plan.
[b]Calculated or estimated values.

Table 3. Aerosol densities and size parameters used for performing LA3 pretest calculations[a,b]

Test	Mixture density (g/cm^3)	Mixed d_{50} (μm)	Mixed d_g (μm)	CsOH d_{50} (μm)	CsOH d_g (μm)	MnO d_{50} (μm)	MnO d_g (μm)
LA3A	2.59	1.24	0.29	1.48	0.35	1.21	0.29
LA3B	2.59	1.24	0.29	1.48	0.35	1.21	0.29
LA3C	2.35	1.30	0.31	1.48	0.35	1.21	0.29

[a]The CsOH theoretical density is 3.68 g/cm^3, and the MnO theoretical density is 5.44 g/cm^3. For each component and for the mixture, the aerosol agglomerate density was assumed to be one-half the theoretical density.

[b]The geometric mean diameter, d_g, was calculated using the formula: $\ln(d_g) = \ln(d_{50}) - 3 \ln^2(\sigma_g)$, using $\sigma_g = 2$.

Table 4. Summary of requested code output parameters for LA3 pretest pipe calculations

Provide the following information for LA3A, LA3B, and LA3C:

Output times (s): 100, 300, 600, 900, 1800, 2700, 3600

Output parameters and units:

A. For each pipe control volume at each output time:

1. Cumulative aerosol mass — for MIXED aerosol and for EACH species — deposited in EACH control volume, in grams. Please provide this for EACH aerosol deposition mechanism that was important — turbulent deposition, deposition in bends, settling, thermophoresis, etc.

2. Airborne aerosol size in EACH control volume — for MIXED aerosol and for EACH species (if possible): provide the aerodynamic mass-median diameter, in μm, and the geometric standard deviation (dimensionless).

B. At pipe outlet, for each output time:

1. Cumulative aerosol mass — for MIXED aerosol and for EACH species — transported out of test pipe, in grams.

2. Airborne aerosol size transported out of test pipe — for MIXED aerosol and for EACH species (if possible): provide the aerodynamic mass-median diameter, in μm, and the geometric standard deviation (dimensionless).

used the same nodalization of the test pipe. Tables 5 and 6 present the LA3B benchmark code input information defined in the guidance letter[3] for this calculation. Finally, Table 7 presents the requested code output parameters for the LA3B benchmark calculation.

3. COMPARATIVE CALCULATIONS OF TURBULENT-DEPOSITION VELOCITIES FOR LA1 AND LA3 TEST CONDITIONS

Aerosol deposition under turbulent flow conditions can occur by essentially two mechanisms: (1) for "small" particles, by diffusion through the turbulent boundary layer and (2) for "large" particles, by diffusion into the boundary layer and subsequent deposition due to particle inertia. For the flow conditions produced in LACE LA1 and LA3, all the aerosol codes used in this study calculated that the majority of aerosol deposition is due to turbulent-inertial deposition. It is instructive, then, to compare the deposition velocity formulations used in the various aerosol-transport codes to calculate turbulent-inertial deposition.

The parameter that characterizes which turbulent-deposition regime is most important is the so-called "dimensionless relaxation time," which is defined as follows:

$$\tau^+ = \frac{\rho_p \rho_g \; d^2 U_*^2 \, C}{18 \; \mu^2 \chi} , \qquad (1)$$

where

ρ_p = particle density,

ρ_g = fluid density,

d = particle diameter,

U_* = fluid friction velocity = $U_f(f/2)^{1/2}$,

U_f = flow velocity through the pipe,

f = flow friction factor,

C = Cunningham slip correction factor,

μ = fluid dynamic viscosity,

χ = dynamic shape factor.

Table 5. Pipe control volume conditions to be used for LA3B pretest benchmark calculation

Control volume	Geometric conditions[a]				Control volume pressure and temperature conditions[b]		
	Pipe sections	Orientation	Length (m)	Sedimentation area (m^2)	Gas pressure (kPa)	Gas temperature (°C)	Wall temperature (°C)
1	4	Vertical	2.26	0.0031	108.9	296	281
2	5-8	Horizontal	5.15	0.324	108.7	283	268
3	9-11	Horizontal	7.28	0.459	108.2	262	247
4	12-14	Horizontal	7.97	0.502	107.7	236	221
5	15-17	Horizontal	2.39	0.151	107.4	218	203
6	18-19	Vertical	2.52	0.0031	107.2	210	195
7	20-21	Horizontal	1.28	0.081	107.1	203	188
8	Aerosol outlet volume						

[a]For all control volumes, the pipe diameter is 0.063 m, and the pipe flow area is 0.0031 m^2.
[b]Estimated conditions.

Table 6. Summary of additional information needed for LA3B pretest benchmark calculation[a]

Test pipe gas flow rates (g/s)			
Steam	12.5		
Nitrogen	18.3		
Helium	0.3		
Argon	0.7		
Volumetric steam fraction	0.5		
Gas mixture viscosity (g/cm-s)	0.00024		
Aerosol source to test pipe (g/s)			
CsOH source rate	0.12		
MnO source rate	1.0		
Aerosol source size parameters:			
Aerodynamic mass-median diameter (μm)	2.0		
Geometric standard deviation	2.0		
Aerosol shape factors	1.0		
Aerosol mixture density (g/cm^3)	2.59[b]		
	Mixed	CsOH	MnO
Mass-median diameter, d_{50} (μm)	1.24	1.48	1.21
Geometric mean diameter, d_g (μm)[c]	0.29	0.35	0.29

[a]Data from LA3 test plan.

[b]The CsOH theoretical density is 3.68 g/cm^3, and the MnO theoretical density is 5.44 g/cm^3. For each component and for the mixture, the aerosol agglomerate density should be assumed to be one-half the theoretical density.

[c]The geometric mean diameter, d_g, was calculated using the formula: $\ln(d_g) = \ln(d_{50}) - 3 \ln^2(\sigma_g)$, using $\sigma_g = 2$.

Table 7. Summary of requested code output parameters for LA3B benchmark pretest calculation

Output time: 3600 s

Output parameters and units for each pipe control volume:

1. Aerosol mass deposited in EACH control volume — for MIXED aerosol and for EACH species, in grams. Please provide this for EACH aerosol deposition mechanism that was important — turbulent deposition, settling, thermophoresis, etc.

2. Calculated deposition velocities for turbulent deposition, deposition by settling, and thermophoretic deposition — in EACH control volume, in cm/s.

3. Aerosol mass transported out of test pipe — for MIXED aerosol and for EACH species, in grams.

4. Airborne aerosol size in EACH control volume — for MIXED aerosol and for EACH species (if possible): provide the aerodynamic mass-median diameter, in μm, and the geometric standard deviation (dimensionless).

Typically, for values of $\tau^+ > 0.1$, inertial effects dominate over pure diffusion. Note from Eq. (1) that this could occur either for large particles or large values of friction velocity (i.e., high Reynolds numbers or flow velocities).

For the LA3 pretest aerosol-transport calculations, three different models for turbulent-inertial deposition were used in the various codes. The first of these was based on an analytical model developed by Friedlander and Johnstone.[4] They were the first to propose that turbulent eddies (from the turbulent core and buffer layer) carry particles to within one "stopping distance" from the wall and that the particles then coast to the wall due to their inertia. The Friedlander-Johnstone model was developed for smooth pipes. Their formulation for deposition velocity depends on the dimensionless relaxation time in the following way:

$$\frac{1}{V_{FJ}} = \left[\frac{1}{(f/2)^{1/2}} + \frac{1525}{0.81\tau^{+2}} - 50.6\right]/U_* \qquad \text{for } \tau^+ < 5.6 \ , \qquad (2)$$

$$\frac{1}{V_{FJ}} = \left[\frac{1}{(f/2)^{1/2}} - 13.73 + 5 \ln \left\{ 5.04 / \left(\frac{\tau^+}{5.56} - 0.959 \right) \right\} \right] / U_* \qquad \text{for } 5.6 < \tau^+ < 33.3 \ , \tag{3}$$

$$V_{FJ} = \left(\frac{f}{2} \right)^{1/2} U_* \qquad \text{for } \tau^+ > 33.3 \ . \tag{4}$$

The formulation for turbulent-inertial deposition velocity used in the TRAP-MELT2 and MCT-2 codes is a modification of the Friedlander-Johnstone model. Gieseke, Lee, and Goldenberg[5] performed experiments in the transition regime between the diffusional and inertial deposition regimes. They found that the Friedlander-Johnstone model does not adequately predict their results, and they included a Reynolds number correction to the Friedlander-Johnstone equations to account for this:

$$V_{FJ,BCL} = V_{FJ} + 2(10^{-8})(Re)\ U_* \ , \tag{5}$$

where Re is the flow Reynolds number.

The model used in the AEROSIM-M calculations is based on a correlation developed by Liu and Agarwal to fit their experimental results.[6] It should be noted that the Liu-Agarwal experiments (the best available data base on turbulent-inertial deposition) were performed at Reynolds numbers of 10,000 and 50,000 and are valid for smooth pipes. The Liu-Agarwal correlation as used in AEROSIM-M calculations is of the form:

$$V_{LA} = 6(10^{-4})\ (\tau^{+2})\ (U_*) \qquad \text{for } \tau^+ < 12.9 \ , \tag{6}$$

$$V_{LA} = 0.1(U_*) \qquad \text{for } \tau^+ > 12.9 \ . \tag{7}$$

The correlation used in the HAA4 aerosol code also was based on the Liu-Agarwal data but was of the following form:[7]

$$V_{LA,HAA4} = [3.03\ (30/\tau^+)^4 + 41.4(\tau^+/30)^{0.342}]^{-1/2} \ . \tag{8}$$

The above correlations were the ones used in the codes for the LA3 pretest calculations. Note, however, that all of these were developed to model deposition onto smooth surfaces. In the LA1 posttest pipe calculations[8] (but not for the LA3 pretest), Battelle-Columbus Laboratories

used a new version of TRAP-MELT — designated as TRAP-MELT2.2 — which included a model for turbulent-inertial deposition onto rough surfaces. This model was developed by Wood[9] and has the following form:[10]

$$V_{WOOD} = \left[\frac{14.5}{(D_p/\nu)^{2/3}}\left\{\frac{1}{6}\ln\left[\frac{(1+F)^2\ (1-F1+F1^2)}{(1+F1^2)\ (1-F+F^2)}\right] + \frac{1}{3^{1/2}}\tan^{-1}\left(\frac{2F-1}{3^{1/2}}\right) - \frac{1}{3^{1/2}}\tan^{-1}\left(\frac{2F1-1}{3^{1/2}}\right) + 24.2\right\}\right]^{-1} U_* \quad \text{for } b_+ + S_+ < 5 , \tag{9}$$

$$V_{WOOD} = U_* \left\{5 \ln \left[25.2/(0.69\tau^+ + 0.45K_+ - 4.8)\right]\right\}^{-1} \quad \text{for } 5 < b_+ + S_+ < 10 , \tag{10}$$

$$V_{WOOD} = 0.129(U_*) \quad \text{for } b_+ + S_+ > 10 , \tag{11}$$

where

$S_+ = 0.69\tau^+$,

$b_+ = 0.45K_+$,

$K_+ = K_s\ U_*/\nu$ = dimensionless surface roughness,

K_s = equivalent sand roughness,

$F = 5/a$,

$F1 = (b_+ + S_+)/a$,

$a = (D_p/\nu)^{1/3}$,

ν = fluid kinematic viscosity,

D_p = particle diffusivity.

Note that this correlation is a function of τ^+ and also of K_+, which is itself a function of the "equivalent sand roughness" that is used to characterize the deposition surface. The relationship in Eq. (11) was determined by the TRAP-MELT 2.2 developers.[10]

Using the deposition model equations presented above [Eqs. (1) to (11)], turbulent-deposition velocities as a function of particle size were calculated for conditions simulating those produced in tests LA1 and LA3. Table 8 presents values of the parameters used in performing these calculations. Two sets of LA1 calculations were performed to model the

Table 8. Summary of parameters used to simulate LA1 and LA3 test conditions[a,b]

Parameter	LA1, low velocity	LA1, high velocity	LA3A	LA3B,C
Particle density (kg/m^3)	3000	3000	3000	3000
Gas density (kg/m^3)	1.23	0.61	0.73	0.57
Gas viscosity (kg/m-s)	2.4E-5	2.4E-5	2.4E-5	2.4E-5
Gas flow rate (kg/s)	0.35	0.35	0.154	0.031
Flow velocity (m/s)	91.6	183.2	67.7	17.4
Flow Reynolds No.	295,000	295,000	130,000	25,900

[a]All calculations were performed for a pipe diameter of 0.063 m. The friction-factor equation used was $f = 0.0014 + 0.125 \times Re^{-0.32}$, where f is the friction factor and Re is the flow Reynolds number.

[b]Wood deposition model calculations were performed using "equivalent sand roughness" values of 1 and 20 μm.

velocity conditions at the inlet and outlet of the pipe. It is interesting to note from Table 8 that the flow Reynolds numbers for tests LA1 and LA3A exceed the values at which deposition measurements were made by Liu and Agarwal.

Figures 1 to 4 present plots of calculated deposition velocities for LA1 and LA3 test conditions. Six deposition-velocity curves are shown on each plot. The ranges of particle diameters used in each graph correspond to a range of dimensionless relaxation times >0.1 and up to 60. Note that on each plot two Wood model curves are shown; these correspond to assumed equivalent sand roughness values of 1 and 20 μm. Comments on the calculated deposition velocity results are as follows:

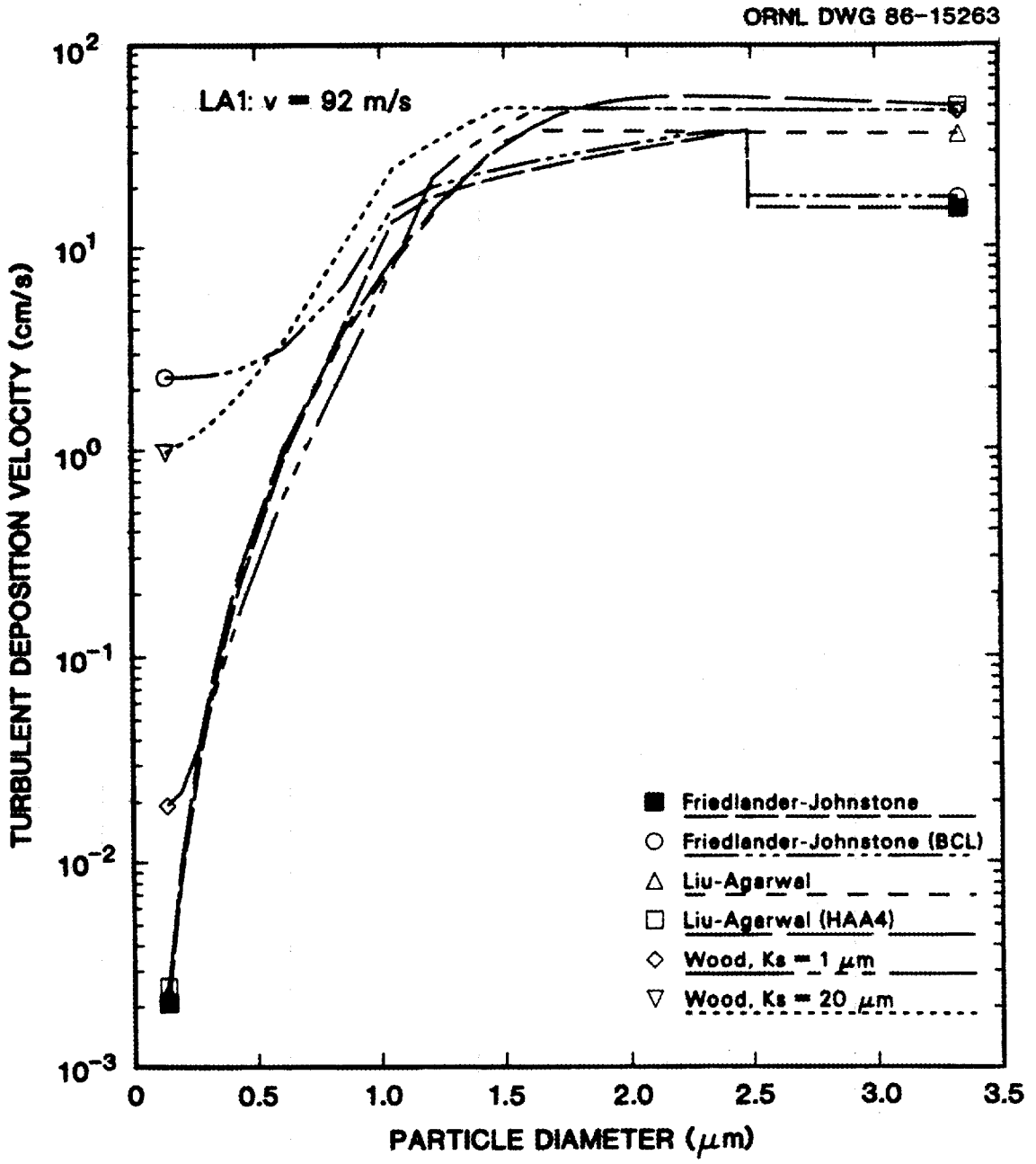

Fig. 1. Comparisons of turbulent-deposition velocities calculated with different models, for test LA1 low-velocity conditions.

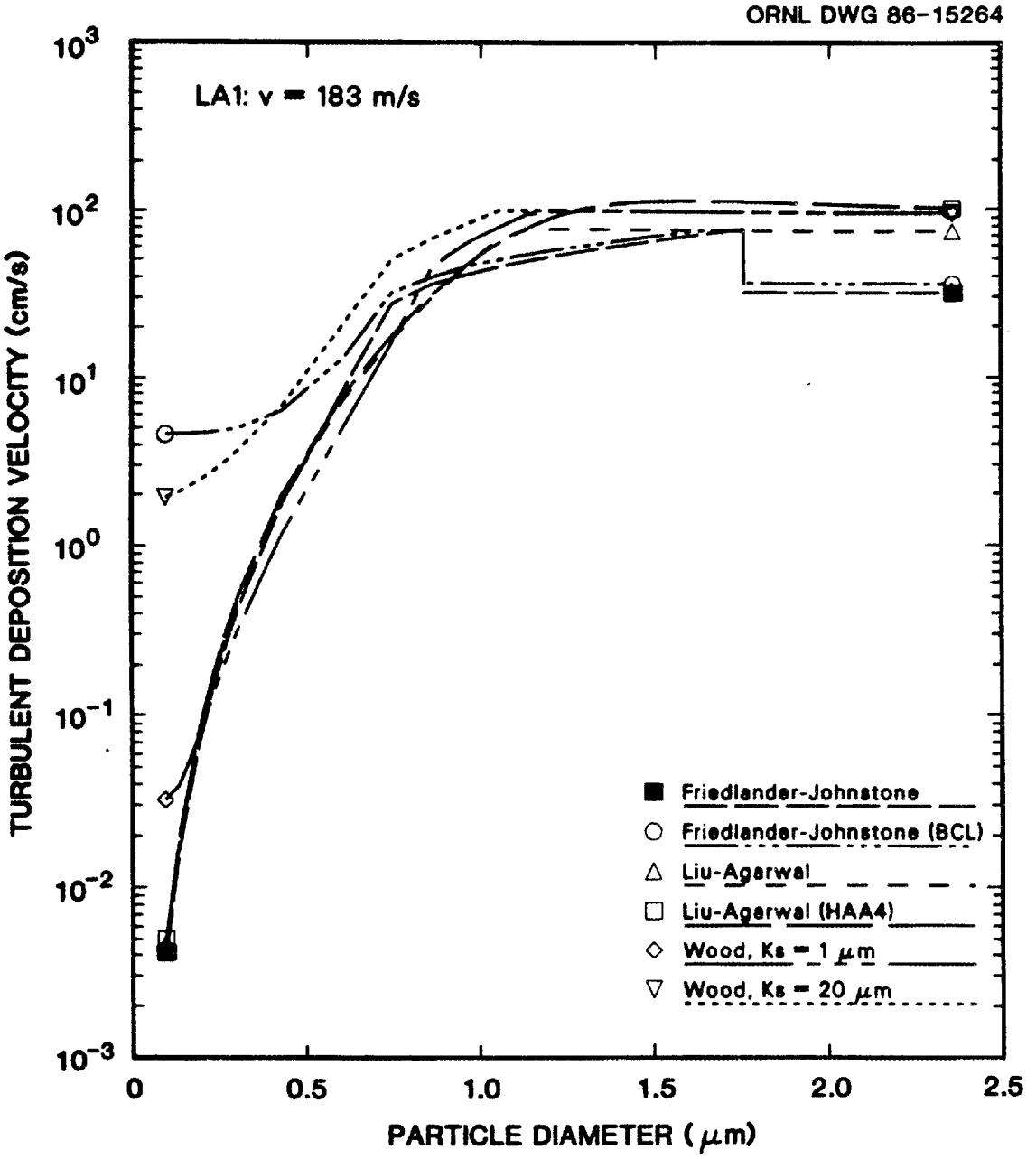

Fig. 2. Comparisons of turbulent-deposition velocities calculated with different models, for test LA1 high-velocity conditions.

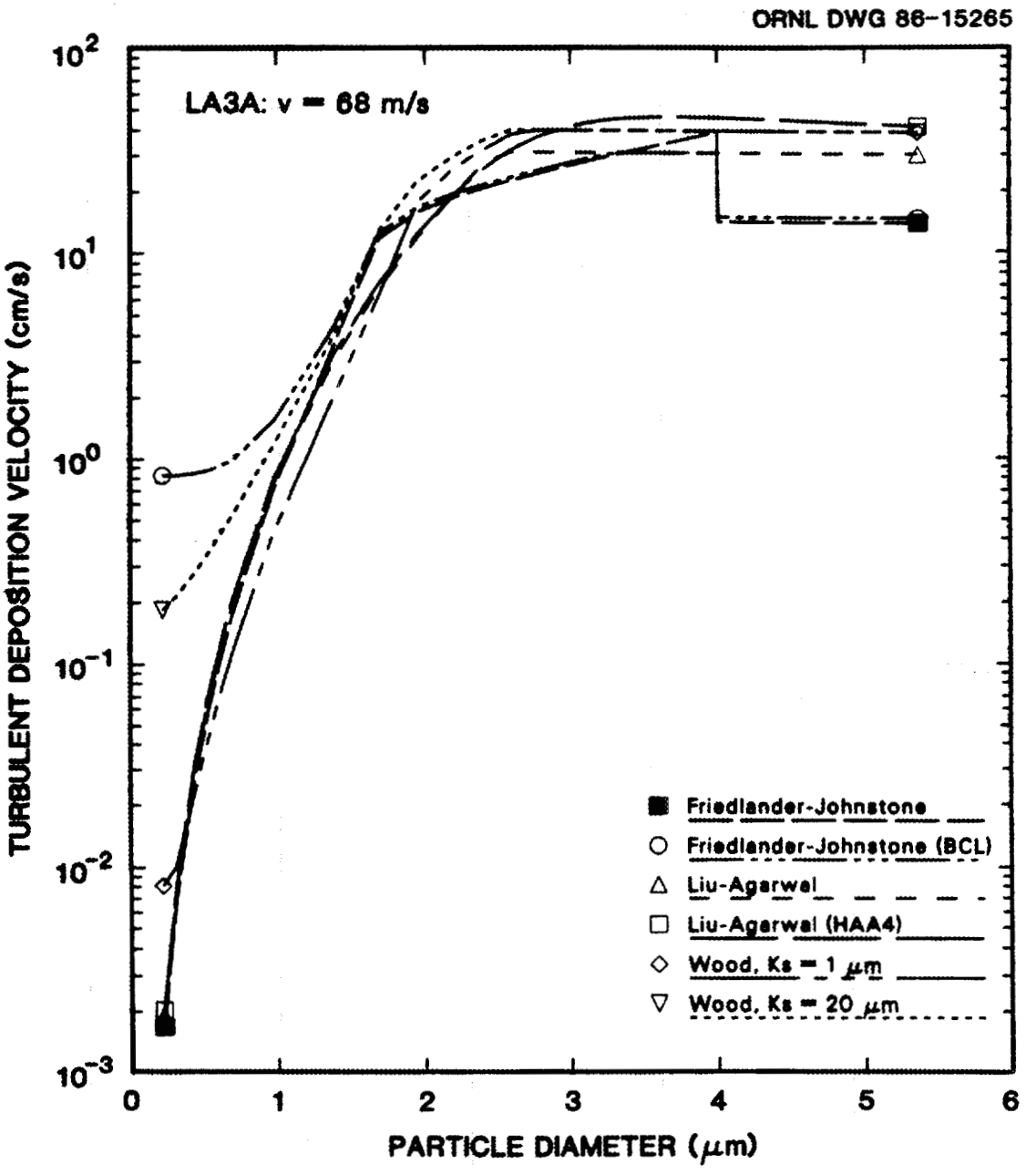

Fig. 3. Comparisons of turbulent-deposition velocities calculated with different models, for test LA3A conditions.

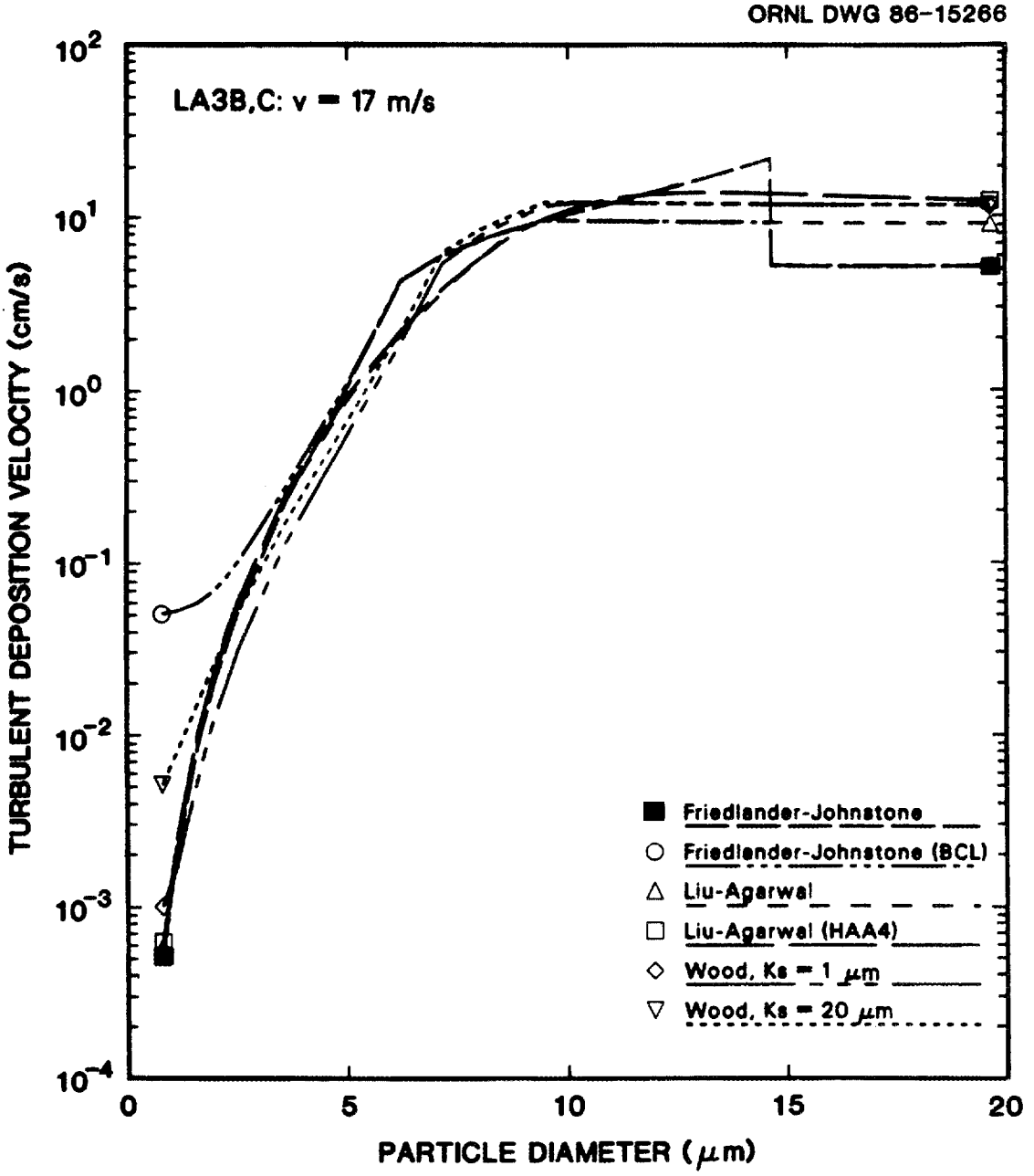

Fig. 4. Comparisons of turbulent-deposition velocities calculated with different models, for test LA3B-LA3C conditions.

1. All results shown illustrate that turbulent-inertial deposition varies significantly with aerosol particle size and with pipe flow velocity, up to "critical" particle sizes corresponding approximately to τ^+ values >10.

2. The correlation of the Liu-Agarwal data used in the HAA4 code [Eq. (8)] models the measured data quite well[7] and can be used (remembering that these data were for smooth tubes) as a basis for comparison with results from other models. Note that the original Liu-Agarwal correlation [Eqs. (6) and (7)] does not match the HAA4 correlation well for large particle-size values.

3. The Friedlander-Johnstone correlation predicts a sharp drop in deposition velocity for values of τ^+ >33.3 [see Eq. (4)]. This dependence is not predicted by the other models and does not correlate with results from the Liu-Agarwal experimental measurements. Because the LACE tests have been performed at high velocities, corresponding to large τ^+ values, this is an important consideration.

4. For small particle sizes (in the transition region between turbulent-inertial deposition and turbulent deposition due to diffusion), the modified Friedlander-Johnstone correlation used in the TRAP-MELT2 code predicts higher deposition velocities than the original Friedlander-Johnstone model. The TRAP-MELT2 version results compare well with results from measurements made at Battelle-Columbus Laboratories[5] but do not match the Liu-Agarwal experimental results.

5. The Wood model results illustrate that, for small particles, calculated deposition velocities increase for increased surface roughness. For an assumed roughness of 1 μm, the Wood model results are similar to those from the HAA4 correlation of the Liu-Agarwal data. It is interesting that, for a roughness of 20 μm, the Wood model results compare reasonably well with those from the modified Friedlander-Johnstone model used in TRAP-MELT2. This suggests the possibility that the Battelle-Columbus experiments were performed with "rough"

tubes; however, smooth-surface copper tubes were used in the experiments.

The main conclusions that can be drawn from evaluation of the different turbulent-inertial deposition models as used in the LA1 and LA3 calculations are as follows: (1) the Friedlander-Johnstone model does not correctly model experimental results for $\tau^+ > 33.3$; (2) the differences between the Liu-Agarwal and Battelle-Columbus test results, for τ^+ values $<\sim 10$, are not understood; (3) the Wood model results show that surface roughness can significantly influence turbulent deposition; and (4) none of the deposition-velocity measurements on which the various correlations and models are based were performed for high enough flow Reynolds numbers to simulate those produced in the LACE LA1 and LA3A experiments.

4. RESULTS FROM INITIAL LA3 PRETEST CALCULATIONS

LA3 pretest pipe calculations were performed by five investigators; the codes used and the names and affiliations of the code analysts are listed in Table 9. The MCT-2 code uses TRAP-MELT2 as a module; so four TRAP-MELT calculations were performed. AEROSIM-M is a containment aerosol-transport code but was used in a "Lagrangian" mode (following an aerosol/gas packet moving down the pipe) for these calculations.

Figures 5 to 16 present the pretest LA3 code results. Plots of cumulative aerosol deposition vs distance from the pipe inlet, at the end of the aerosol source period (3600 s), are presented in Figs. 5 to 7. Figures 8 to 10 present calculated aerosol transport out of the pipe vs time. Finally, Figs. 11 to 16 present calculated aerodynamic mass-median diameter (AMMD) and geometric standard deviation data vs distance from the pipe inlet, at 3600 s.

Figures 5 to 7 illustrate that the agreement in calculated deposition results was better for LA3A than for LA3B and LA3C. The variation in total calculated deposition for LA3A was less than a factor of 2 but was more than a factor of 6 for LA3B and LA3C. Tables 10 and 11 provide information that can be used to explain differences in calculated code results. Comments on the code results and data in the tables are as follows:

Table 9. Summary of codes used for LA3 pretest pipe calculations

Code[a]	Code analyst	Affiliation
AEROSIM-M (UK)	S. Ramsdale	United Kingdom, Atomic Energy Authority, Safety and Reliability Directorate
MCT-2 (NYPA)	P. Bieniarz	United States, New York Power Authority
TRAP-MELT2 (IT)	F. Parozzi	Italy, ENEL-Thermal and Nuclear Research Centre
TRAP-MELT2 (JN)	H. Tateoka	Japan, Atomic Energy Research Institute
TRAP-MELT2 (UK)	D. Williams	United Kingdom, Atomic Energy Authority, AEE Winfrith

[a]Initials in parentheses indicate the country or organization.

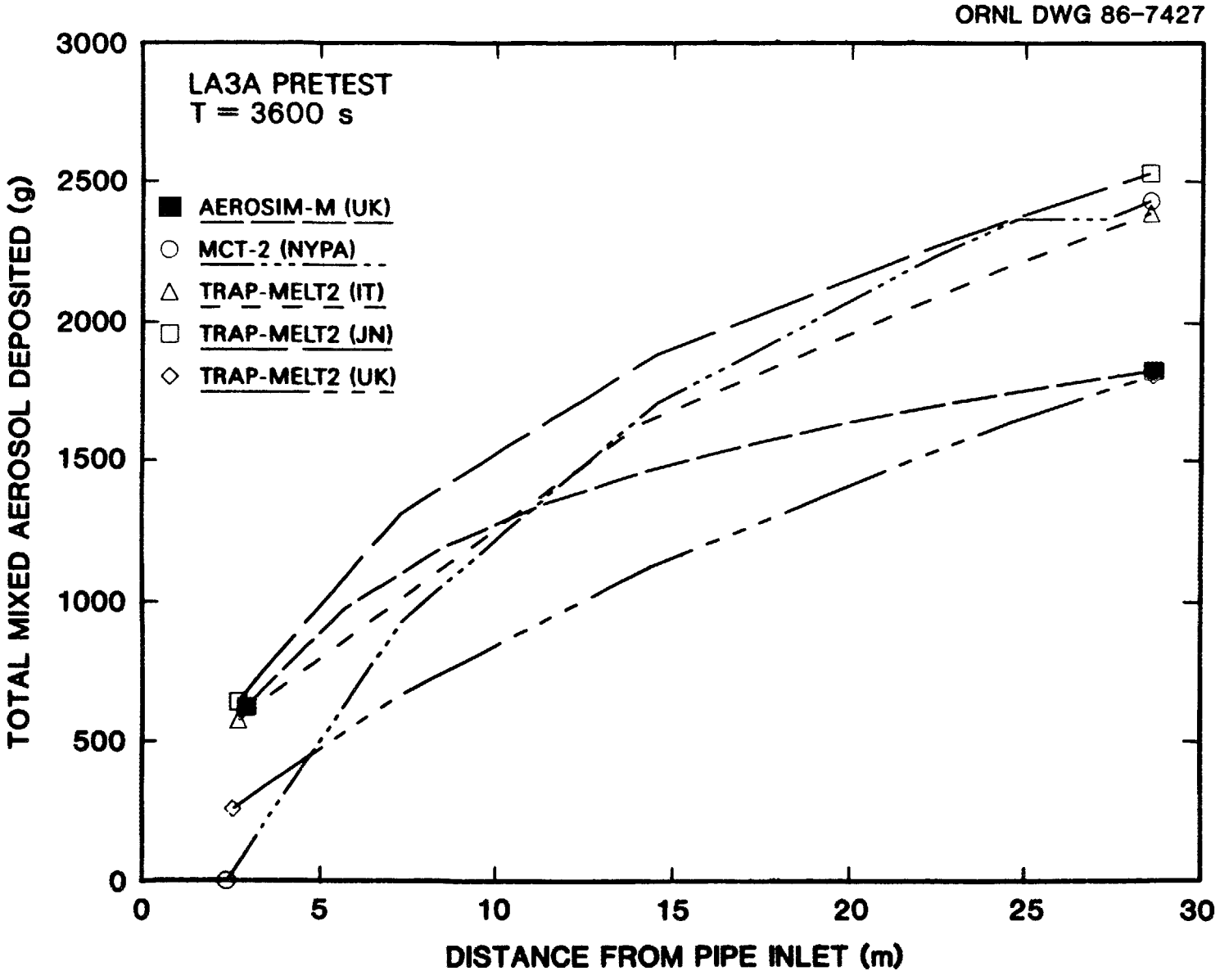

Fig. 5. LA3A pretest results: total aerosol deposited in pipe vs distance from pipe inlet, at t = 3600 s.

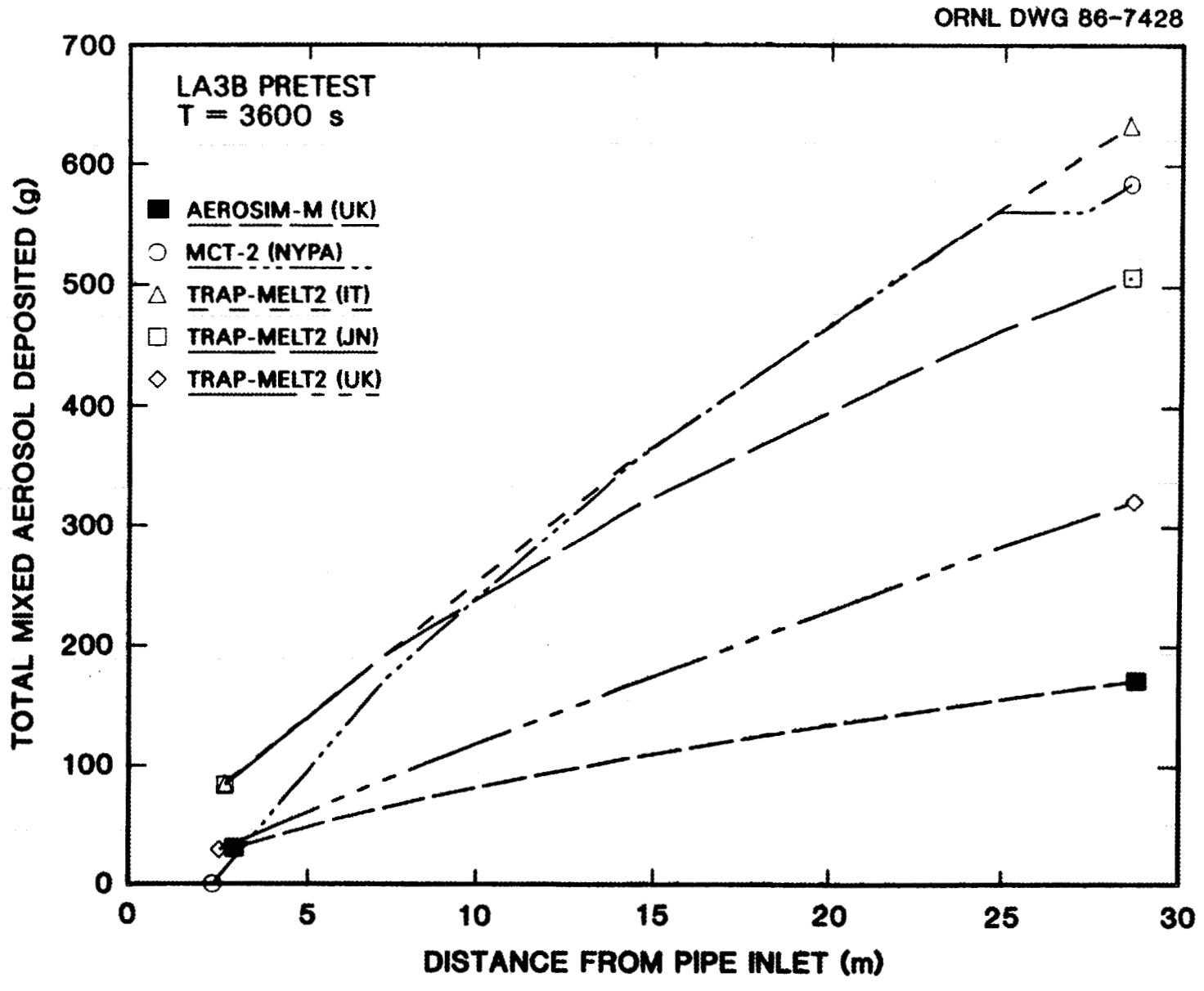

Fig. 6. LA3B pretest results: total aerosol deposited in pipe vs distance from pipe inlet, at t = 3600 s.

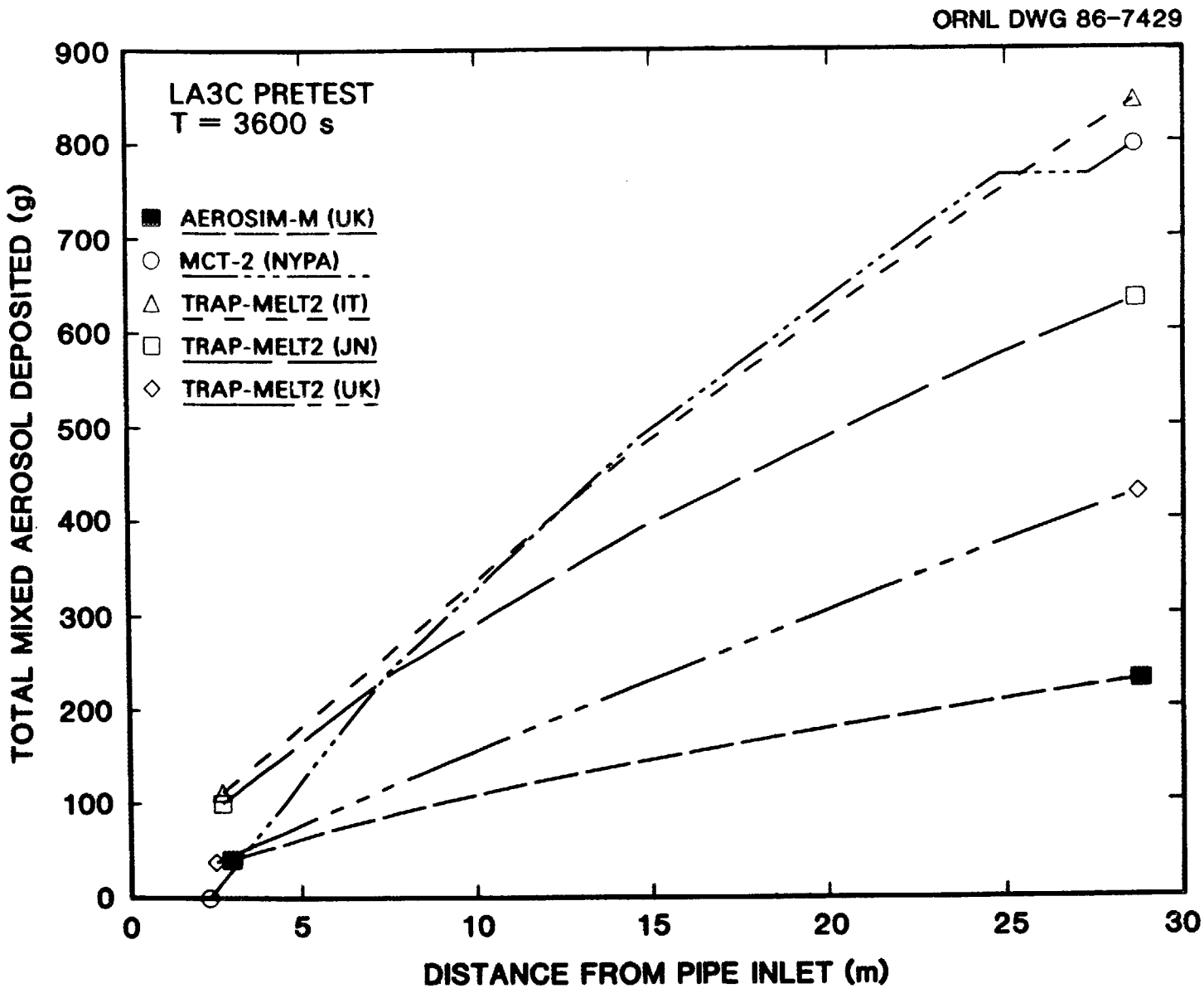

Fig. 7. LA3C pretest results: total aerosol deposited in pipe vs distance from pipe inlet, at t = 3600 s.

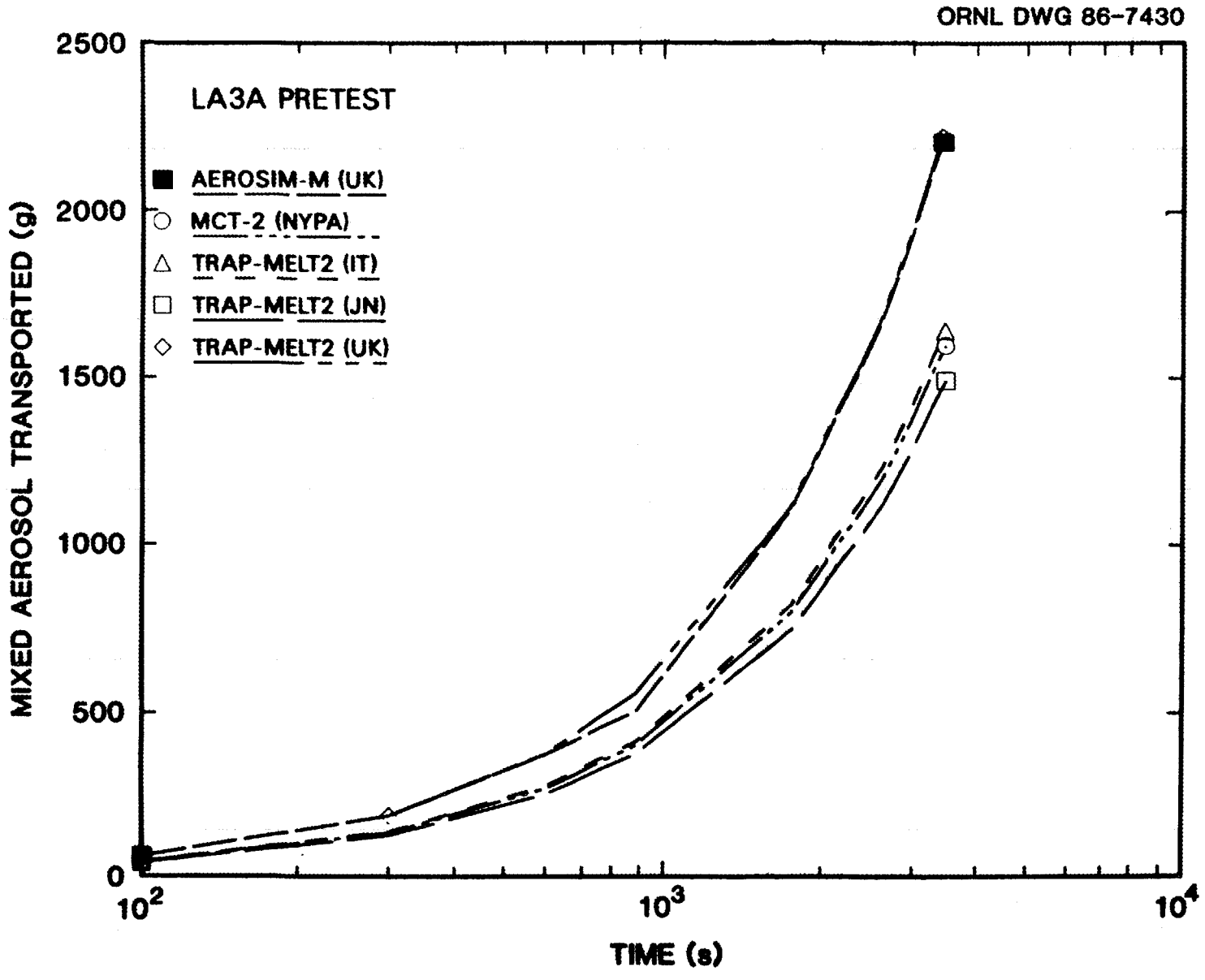

Fig. 8. LA3A pretest results: total aerosol transported out of pipe vs time.

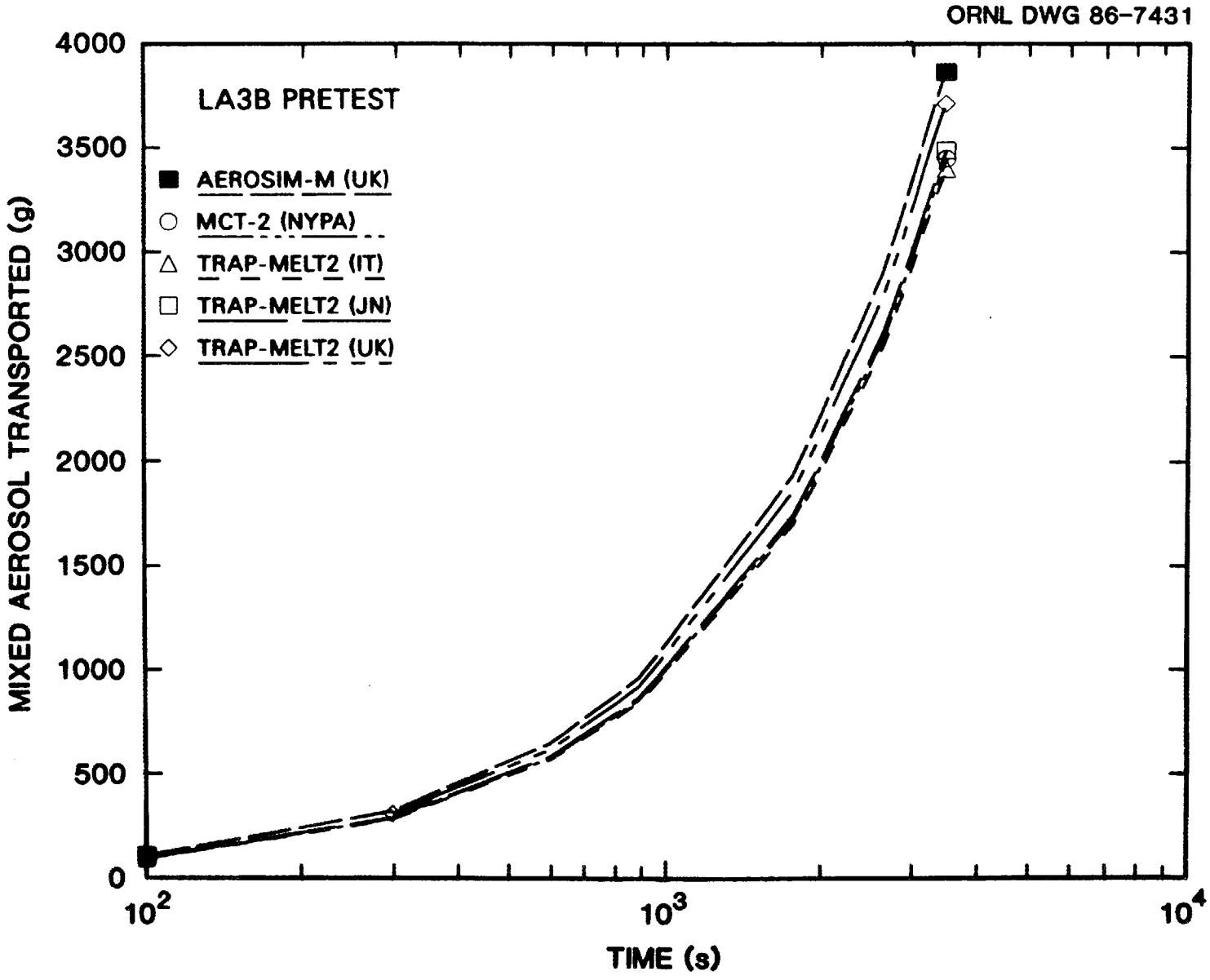

Fig. 9. LA3B pretest results: total aerosol transported out of pipe vs time.

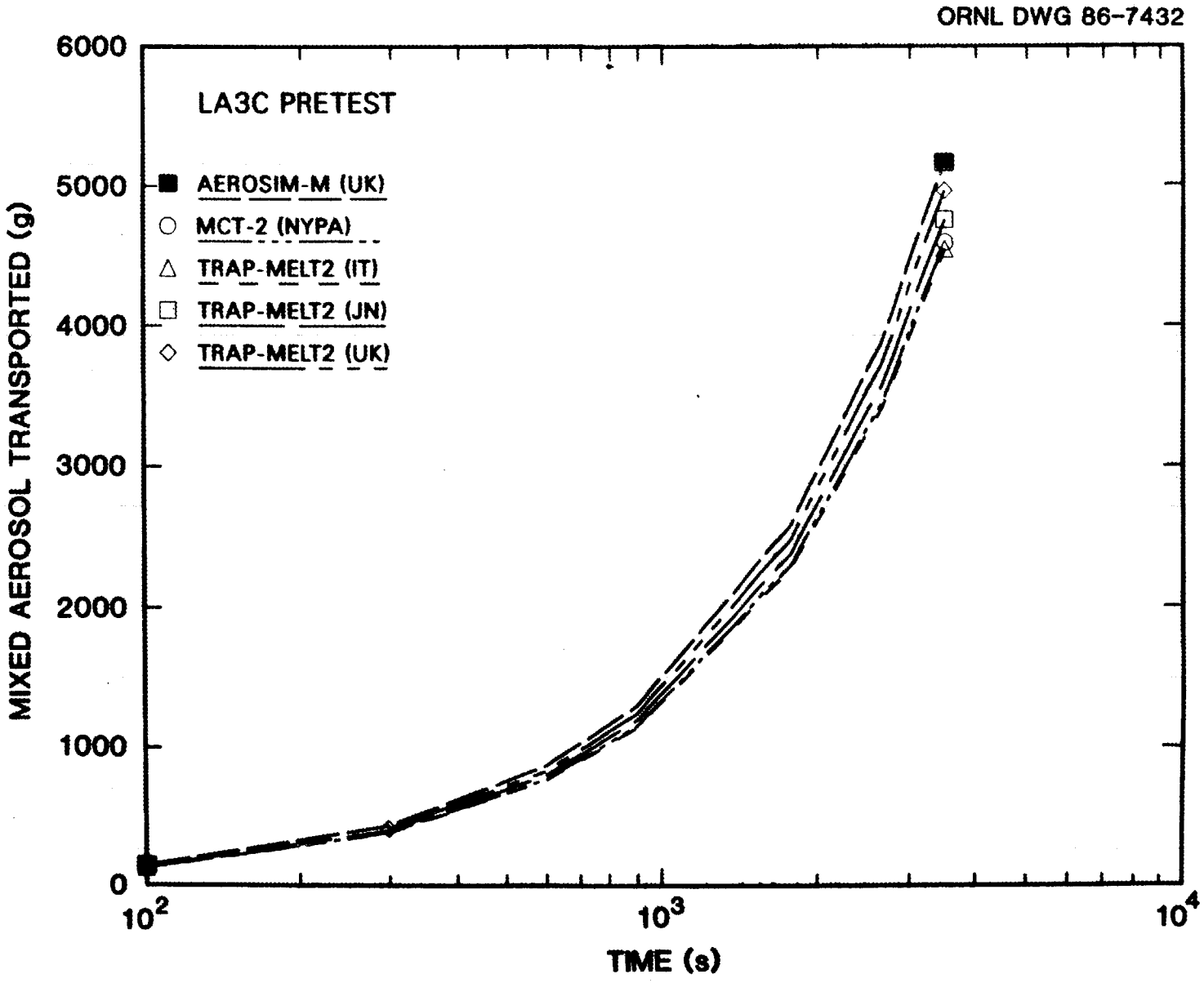

Fig. 10. LA3C pretest results: total aerosol transported out of pipe vs time.

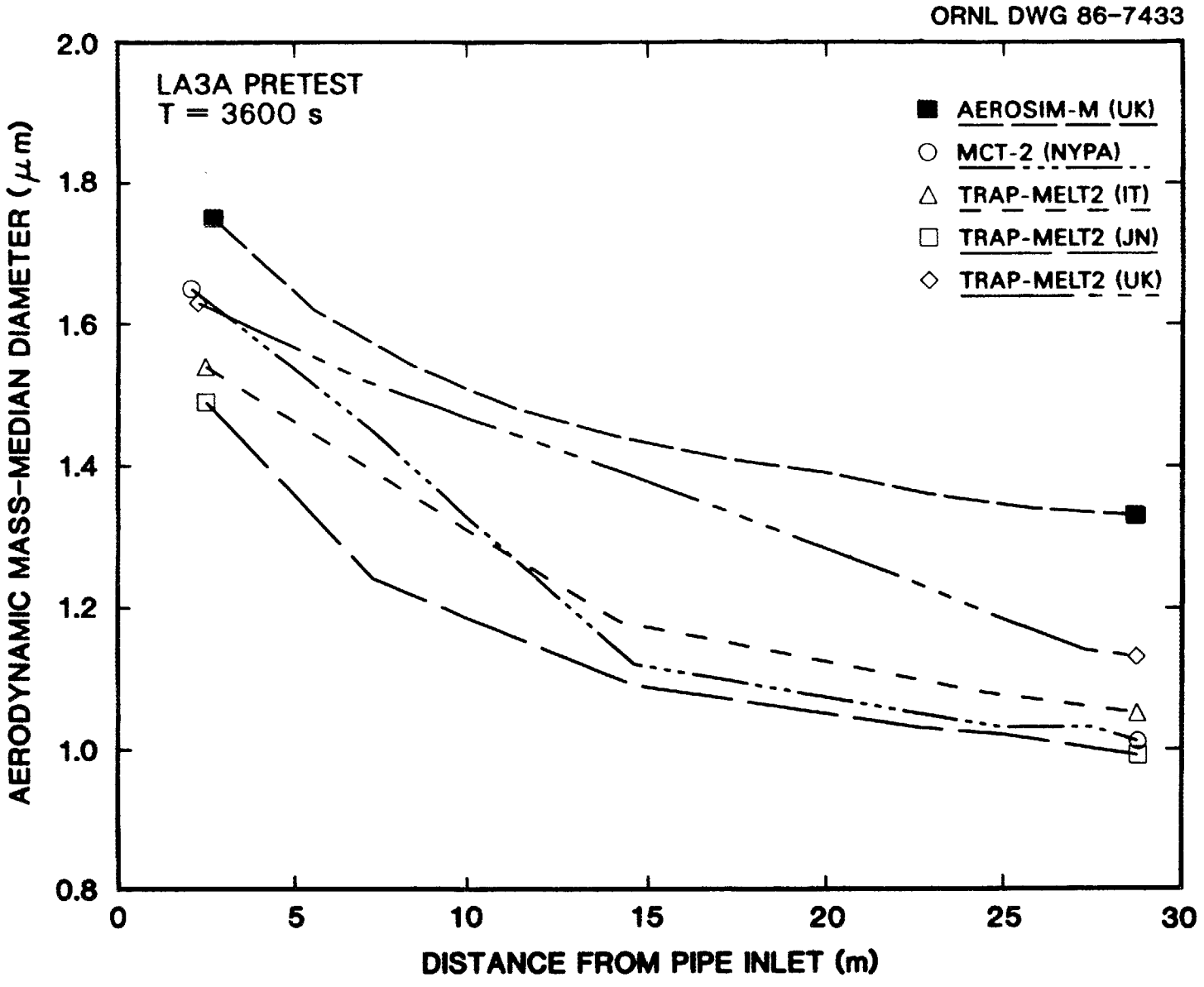

Fig. 11. LA3A pretest results: aerodynamic mass-median diameter vs distance from pipe inlet, at t = 3600 s.

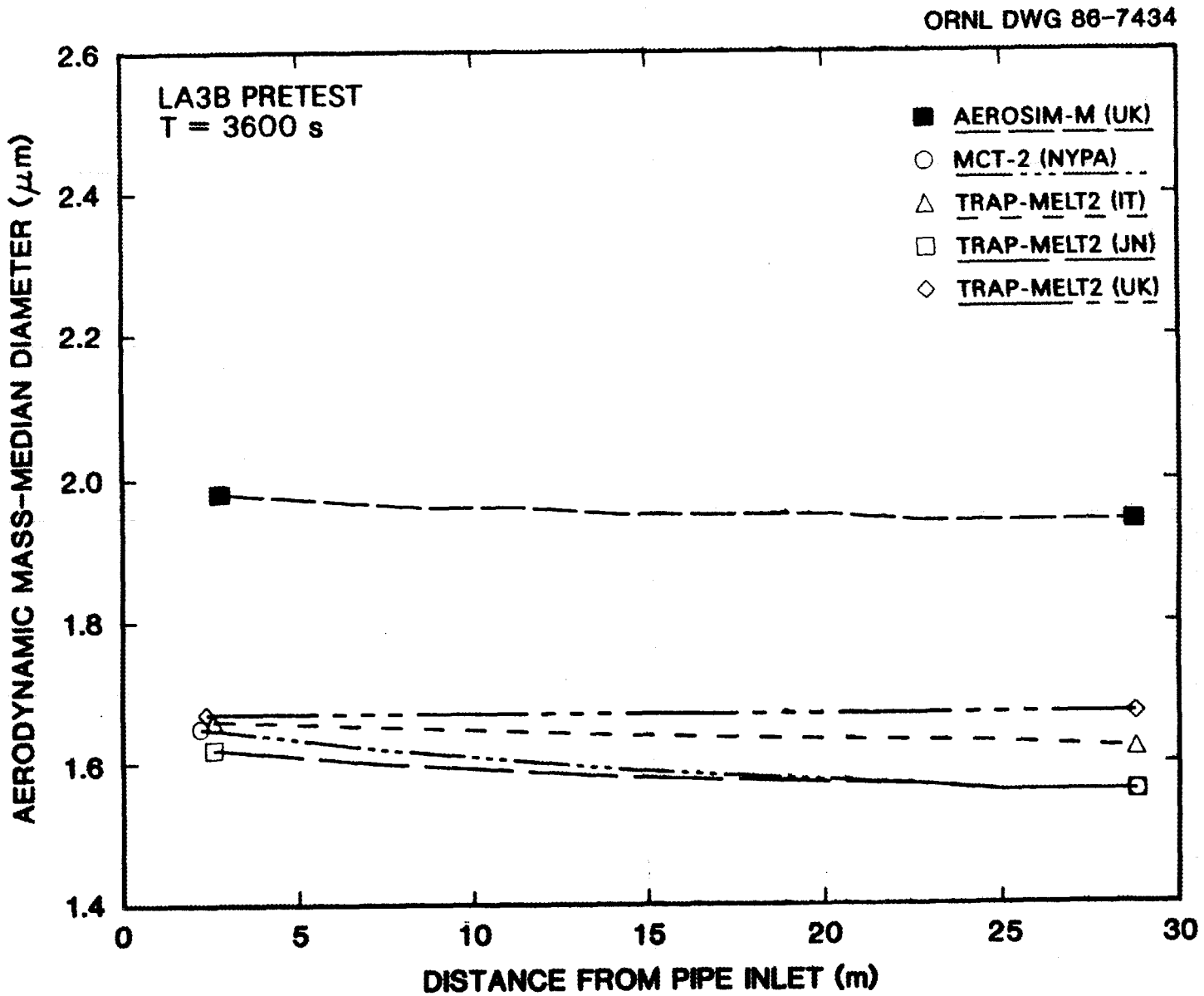

Fig. 12. LA3B pretest results: aerodynamic mass-median diameter vs distance from pipe inlet, at t = 3600 s.

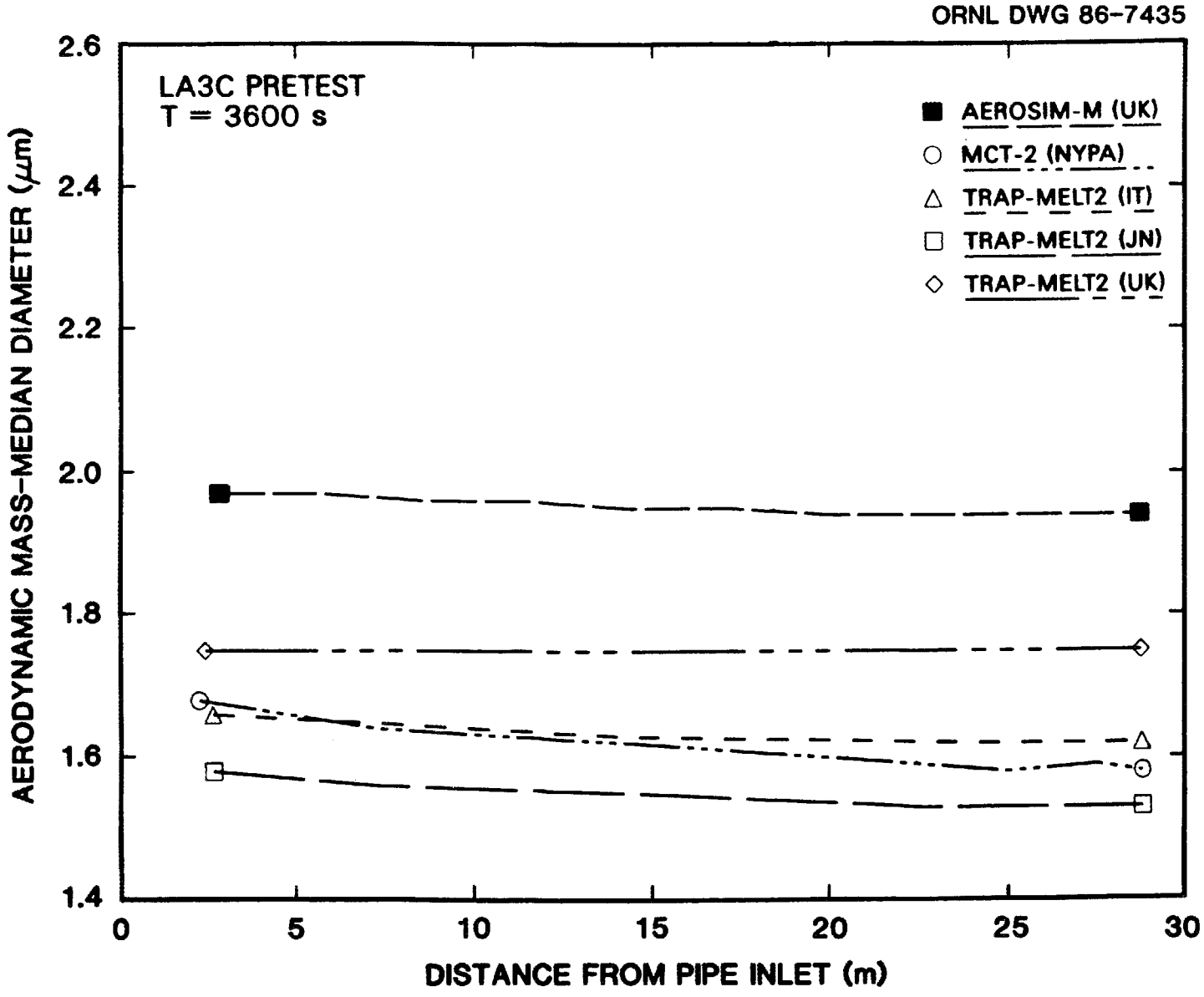

Fig. 13. LA3C pretest results: aerodynamic mass-median diameter vs distance from pipe inlet, at t = 3600 s.

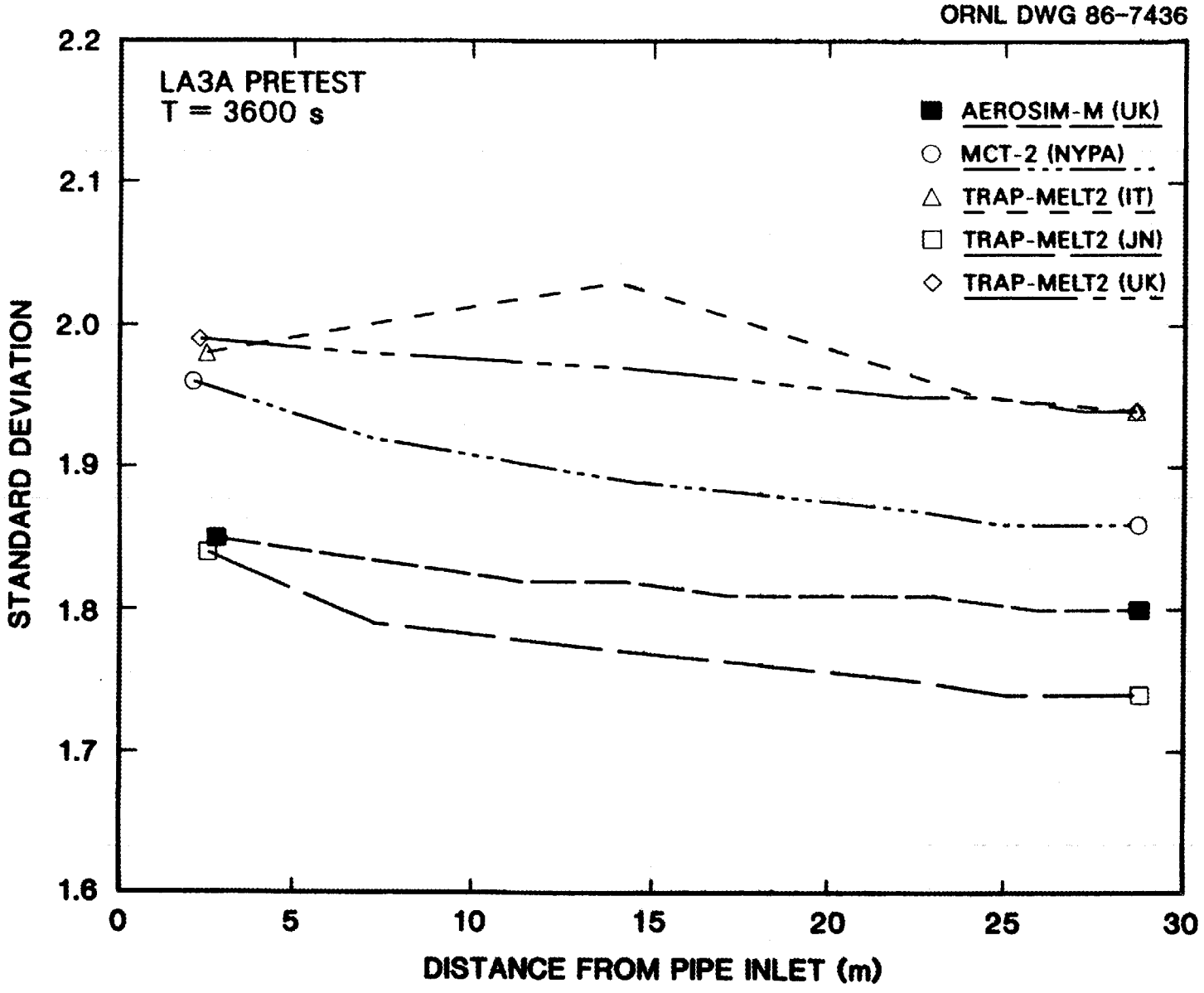

Fig. 14. LA3A pretest results: geometric standard deviation vs distance from pipe inlet, at t = 3600 s.

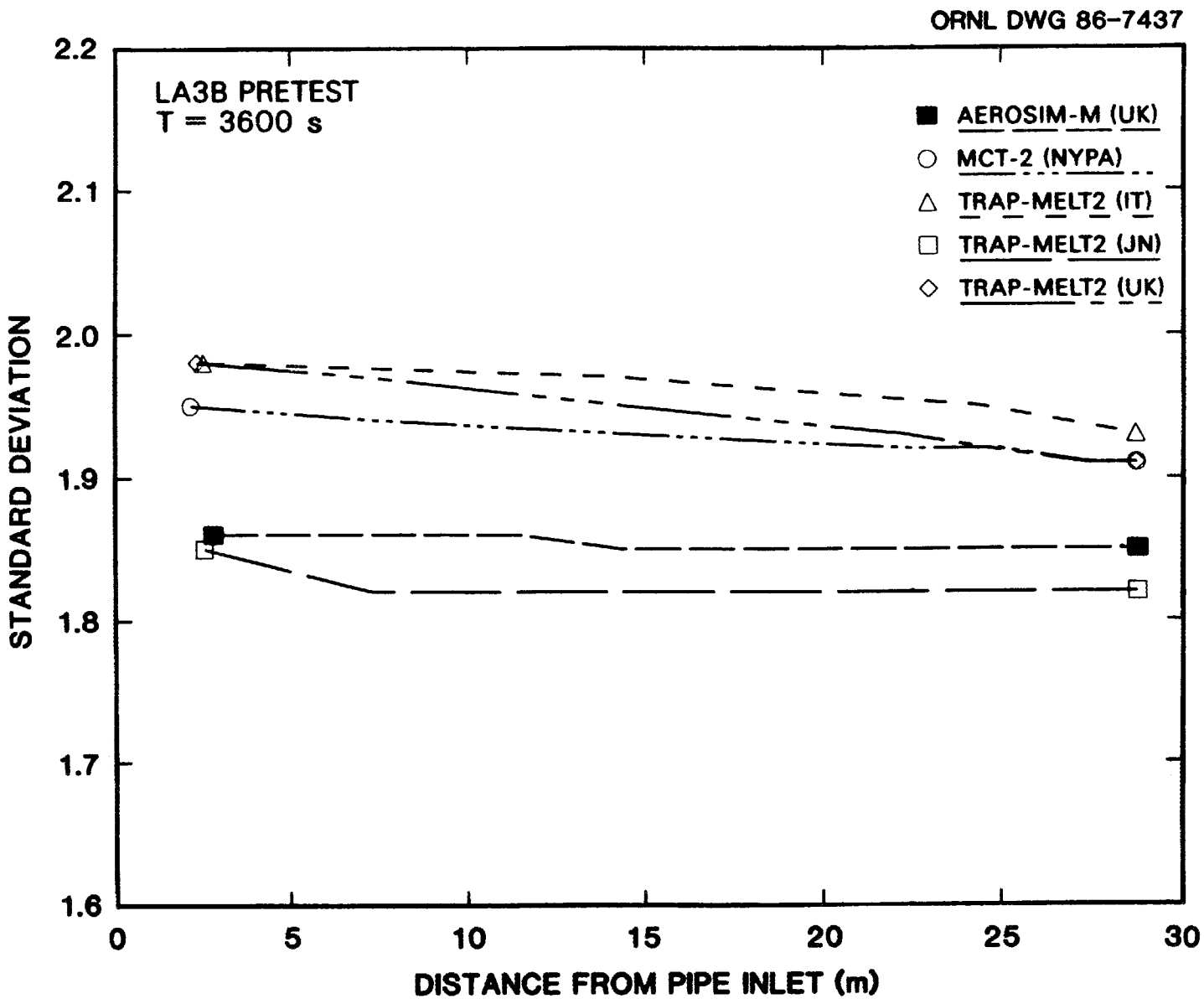

Fig. 15. LA3B pretest results: geometric standard deviation vs distance from pipe inlet, at t = 3600 s.

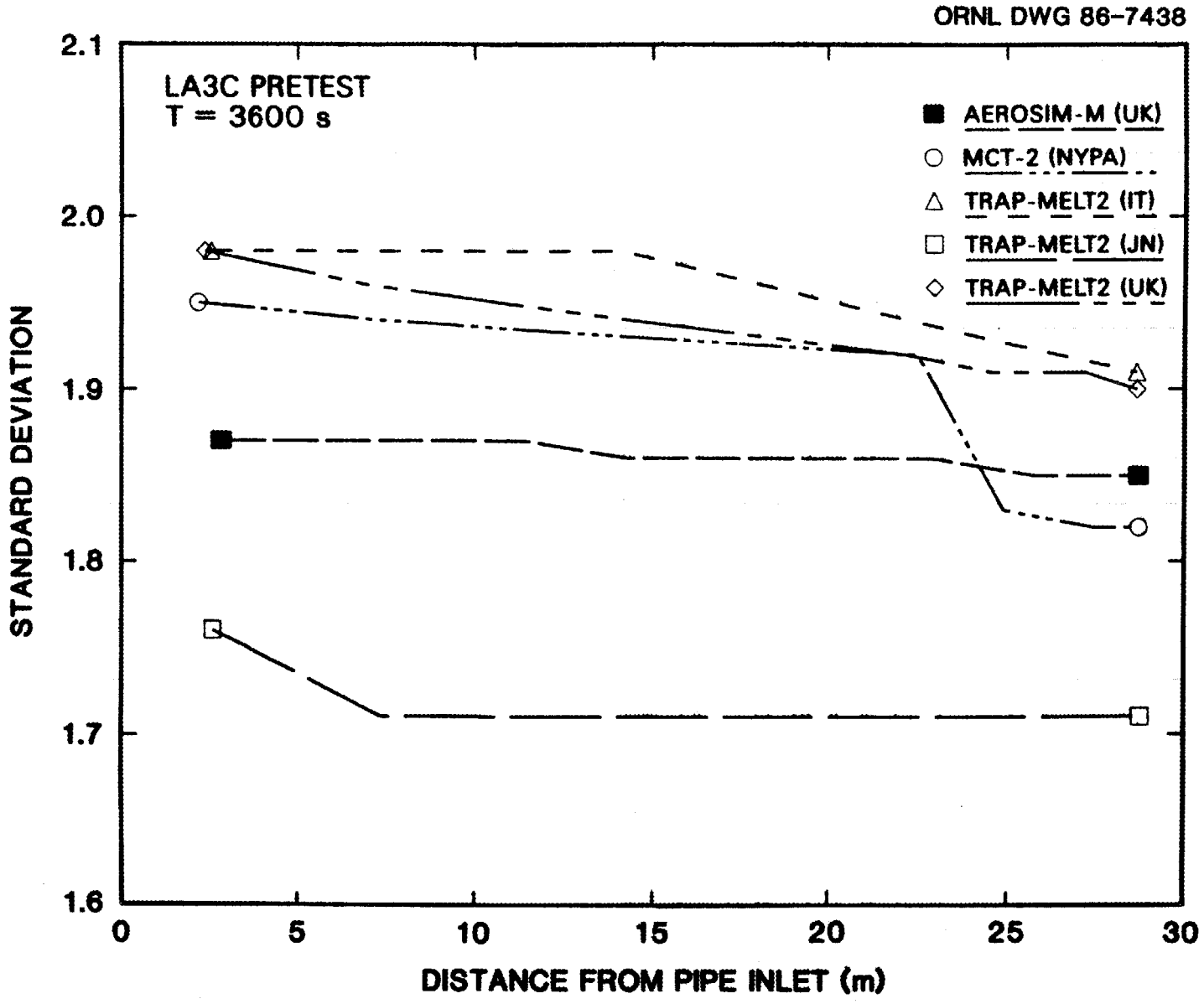

Fig. 16. LA3C pretest results: geometric standard deviation vs distance from pipe inlet, at t = 3600 s.

Table 10. Comparison of selected parameters from LA3 pretest calculations

Code	Range of calculated carrier-gas density (kg/m^3)	Range of calculated carrier-gas viscosity (kg/m-s)	Range of calculated carrier-gas flow velocity (m/s)	Range of calculated turbulent-deposition velocity (cm/s)
		LA3A		
AEROSIM-M (UK)	0.73	2.4E-5	67.7	a
MCT-2 (NYPA)	0.66	2.0E-5	73.3	6.7-3.7
TRAP-MELT2 (IT)	0.83-0.64	2.4-2.3E-5	61.5-79.5	6.1-3.5
TRAP-MELT2 (JN)	a	a	a	10.0-5.2
TRAP-MELT2 (UK)	0.81-0.61	2.5-2.4E-5	48.6-64.3	2.7-2.3
		LA3B		
AEROSIM-M (UK)	0.57	2.4E-5	17.4	a
MCT-2 (NYPA)	0.42	2.0E-5	24.3	0.31-0.19
TRAP-MELT2 (IT)	0.53-0.62	2.4-2.1E-5	20.2-17.4	0.21-0.11
TRAP-MELT2 (JN)	a	a	a	0.36-0.12
TRAP-MELT2 (UK)	0.51-0.60	2.5-2.1E-5	15.8-13.4	0.079-0.059
		LA3C		
AEROSIM-M (UK)	0.57	2.4E-5	17.4	a
MCT-2 (NYPA)	0.42	2.0E-5	24.3	0.32-0.20
TRAP-MELT2 (IT)	0.53-0.62	2.4-2.1E-5	20.2-17.4	0.21-0.11
TRAP-MELT2 (JN)	a	a	a	0.32-0.12
TRAP-MELT2 (UK)	0.51-0.60	2.5-2.1E-5	15.8-13.4	0.079-0.059

[a]Data not provided for this parameter.

Table 11. Calculated deposition, by mechanism, for LA3 pretest calculations

Code	Calculated turbulent deposition (g)	Calculated deposition by thermophoresis plus settling (g)	Calculated deposition by thermophoresis (g)	Calculated deposition by settling (g)
		LA3A		
AEROSIM-M (UK)	1829	0		
MCT-2 (NYPA)	2430	6		
TRAP-MELT2 (IT)	2366	25		
TRAP-MELT2 (JN)	2504	29		
TRAP-MELT2 (UK)	1795	18		
		LA3B		
AEROSIM-M	171	0	0	0
MCT-2 (NYPA)	552	32	16	16
TRAP-MELT2 (IT)	457	175	156	19
TRAP-MELT2 (JN)	317	189	5	184
TRAP-MELT2 (UK)	251	69	45	24
		LA3C		
AEROSIM-M	230	0	0	0
MCT-2 (NYPA)	754	44	21	23
TRAP-MELT2 (IT)	612	230	205	25
TRAP-MELT2 (JN)	395	239	7	232
TRAP-MELT2 (UK)	337	92	60	32

1. Table 10 shows that the TRAP-MELT2 (UK) flow velocities and turbulent-deposition velocities were lower than those calculated by other codes. This occurred because the pipe flow area used in the UK calculations was too large by roughly 30%. This led to calculation of low values of turbulent deposition by the TRAP-MELT2 (UK) code. When this was corrected (too late to modify this report), the calculated total amounts of deposition were 2379 g for LA3A, 518.2 g for LA3B, and 698.3 g for LA3C. These are much closer to the amounts of deposition calculated by other TRAP-MELT users.

2. By hand calculations, we confirmed that the mixture density values used in the (UK) and (IT) TRAP-MELT2 calculations were correct. The values of density and viscosity used in the MCT-2 calculations were lower than the British and Italian values. This caused the code to calculate higher velocities, higher τ^+ values [see Eq. (1)], and therefore higher turbulent-deposition velocities.

3. In the MCT-2 calculations, aerosol deposition in the two vertical sections of the pipe was not allowed (by setting one of the code input parameters to zero). Had deposition been allowed in these sections, we believe that MCT-2 would have calculated more overall deposition than did the other codes.

4. Table 11 illustrates that, for the tests with lower flow velocities (LA3B and LA3C), the contribution of settling and thermophoresis to the total deposition became important. For all LA3A calculations, turbulent deposition accounted for about 99% of the total calculated deposition. For LA3B and LA3C, however, thermophoresis plus settling accounted for as much as 20 to 30% of the total calculated deposition. Note that no settling or thermophoretic deposition was allowed in the AEROSIM-M calculations; we believe that deposition by these mechanisms should be included for the posttest calculations.

5. For LA3B and LA3C, TRAP-MELT2 (IT) calculated the greatest amount of thermophoretic deposition, while TRAP-MELT2 (JN) calculated the greatest amount of settling. However, the (JN) calculations assumed that the settling deposition area was $\Pi \cdot d \cdot l$, where d is the pipe

diameter and l is the control volume length. The correct settling area to use is d·l; therefore, the (JN) settling values are about a factor of 3 larger than they should be.

6. The results in Table 11 show that AEROSIM-M tended to predict the least amount of turbulent deposition. The deposition-velocity comparisons in Fig. 4 (for LA3B, LA3C conditions) suggest that this occurred because of differences in the Liu-Agarwal correlation and the Battelle-Columbus version of the Friedlander-Johnstone correlation. Figure 4 shows that, of these two correlations, the Liu-Agarwal correlation predicts significantly lower deposition velocities for particles <3 to 4 μm in diameter.

Although there were significant differences in calculated deposition patterns for the LA3 tests, Figs. 8 to 10 show that all codes calculated similar amounts of aerosol leakage vs time. Calculated differences were greater for LA3A because the fractional leakage for LA3A conditions was less than that for LA3B and LA3C.

As shown in Figs. 11 to 13, all codes predicted that the airborne AMMD would decrease as the aerosol flows through the pipe. This decrease is expected since turbulent deposition is more effective for larger aerosol particles. The results also show that the calculated rate of decrease of AMMD is greater for LA3A, which had the higher flow velocity. Possible causes for this are (1) the reduced deposition of larger particles for the lower gas velocity conditions in LA3B and LA3C (Figs. 3 and 4) and (2) increased aerosol agglomeration for the longer flow residence times in LA3B and LA3C.

The LA3B and LA3C AMMD values for the TRAP-MELT (including MCT-2) calculations are significantly less than those calculated by AEROSIM-M. As was discussed and confirmed in the LA2 pretest[11] and LA1 posttest[8] reports, the TRAP-MELT code does not correctly calculate the AMMD from the code size-distribution data. We believe that this caused the observed differences.

Except for the TRAP-MELT2 (IT) results, the standard deviation data in Figs. 14 to 16 show that σ_g decreases with distance from the pipe inlet.

We cannot explain why the TRAP-MELT2 (IT) σ_g values increase and then decrease with distance from the pipe inlet. The sharp drop in σ_g near the pipe outlet for the MCT-2 LA3C calculation also cannot be explained.

5. RESULTS FROM LA3B BENCHMARK CALCULATIONS

The results in Sect. 4 illustrated that similar TRAP-MELT2 results were not obtained when different investigators used the code to perform LA3B and LA3C calculations. The LA3B benchmark calculation was performed to investigate what results would be obtained when all investigators used the same nodalization of the test pipe and the same pipe pressure and temperature conditions in their calculations.

LA3 benchmark pipe calculations were performed by five investigators; the codes used and the names and affiliations of the code analysts are listed in Table 12. Three TRAP-MELT calculations (including the

Table 12. Summary of codes used for LA3 pretest benchmark pipe calculations

Code[a]	Code analyst	Affiliation
AEROSIM-M (UK)	S. Ramsdale	United Kingdom, Atomic Energy Authority, Safety and Reliability Directorate
HAA4 (RI)	E. Vaughan	United States, Rockwell International
MCT-2 (NYPA)	P. Bieniarz	United States, New York Power Authority
TRAP-MELT2 (JN)	H. Tateoka	Japan, Atomic Energy Research Institute
TRAP-MELT2 (UK)	D. Williams	United Kingdom, Atomic Energy Authority, AEE Winfrith

[a]Initials in parentheses indicate the country or organization.

MCT-2 one) were performed, and AEROSIM-M was also again used. In addition, a calculation with a version of the HAA4 code modified for use in analysis of flow through pipes was performed. The HAA4 code is a log-normal particle-size distribution containment aerosol code. It was modified so that it could be used to calculate the lengthwise variation of aerosol deposition in a pipe, under the assumption that no aerosol agglomeration occurred as aerosol moved through the pipe. For the HAA4 calculations, then, deposition is the mechanism by which the airborne size distribution changes.

Figures 17 to 20 illustrate the major results from the LA3B benchmark calculations. Similar to what was presented in Sect. 4, Table 13 presents a summary of selected parameters from the calculations, and Table 14 presents calculated aerosol deposition by mechanism. The following comments can be made about the results:

1. Figures 17 and 18 show that the agreement in calculated aerosol deposition for the TRAP-MELT runs was much improved for the benchmark calculation. This occurred largely because the flow area error in the TRAP-MELT2 (UK) calculation was corrected. Figure 18 shows the calculated deposition in each of the pipe control volumes and again indicates agreement in the TRAP-MELT2 deposition calculations.

2. Tables 13 and 14 illustrate an inconsistency in the TRAP-MELT2 (JN) results. Ignoring the AEROSIM-M results, the (JN) calculation had the least amount of turbulent deposition (Table 14); however, the values of turbulent-deposition velocity quoted in Table 13 were the largest. We can only speculate that the deposition velocities provided to us were incorrect. We should note, as was discussed in Sect. 4, that, again, the (JN) calculation used an incorrect equation for determining the settling area and thus overcalculated settling by about a factor of 3.

3. As for the previous LA3B calculations, AEROSIM-M calculated the least amount of turbulent deposition. However, the HAA4 calculation, which used a different correlation to the Liu-Agarwal turbulent-deposition

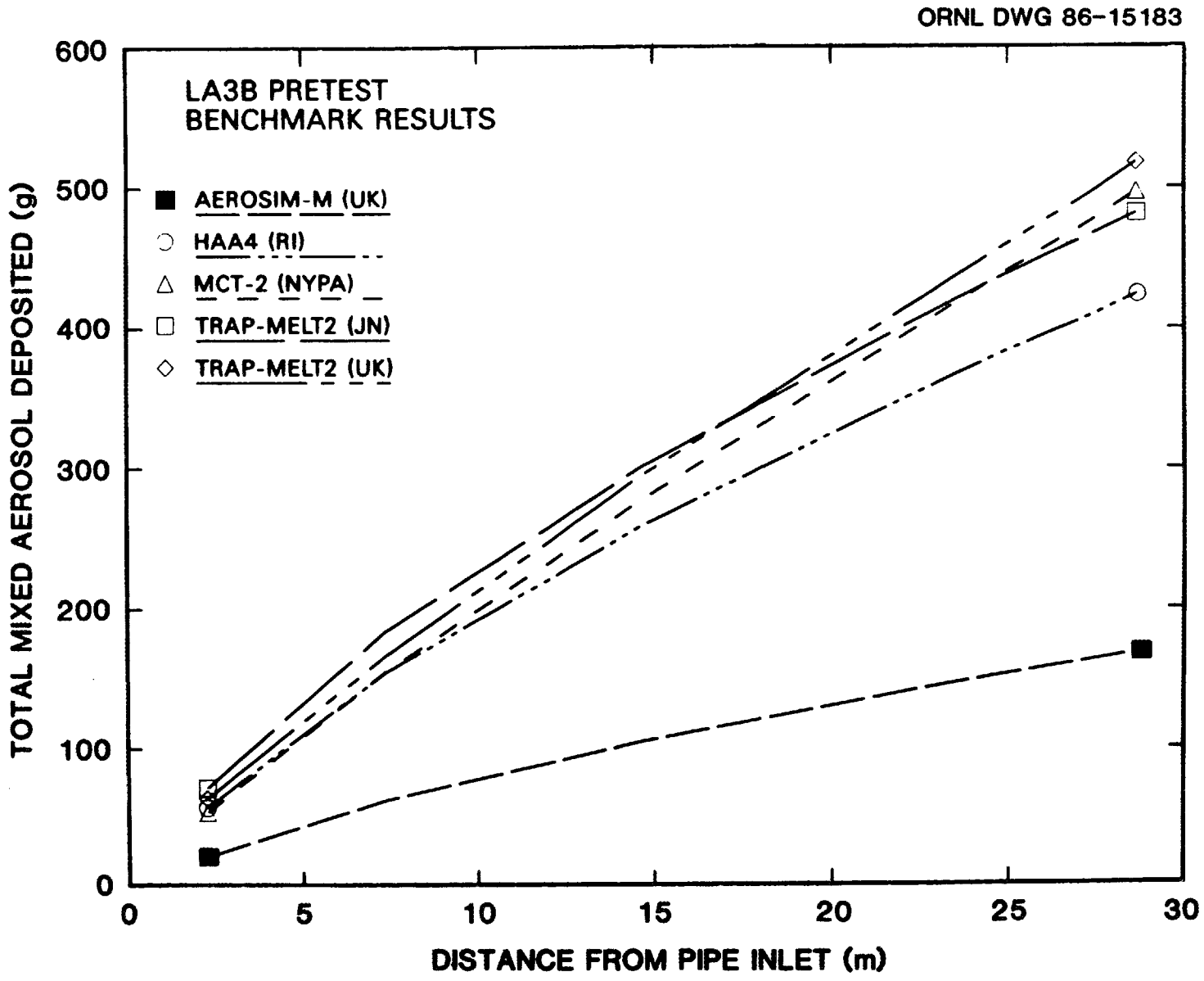

Fig. 17. LA3B benchmark pretest results: total aerosol deposited in pipe vs distance from pipe inlet, at t = 3600 s.

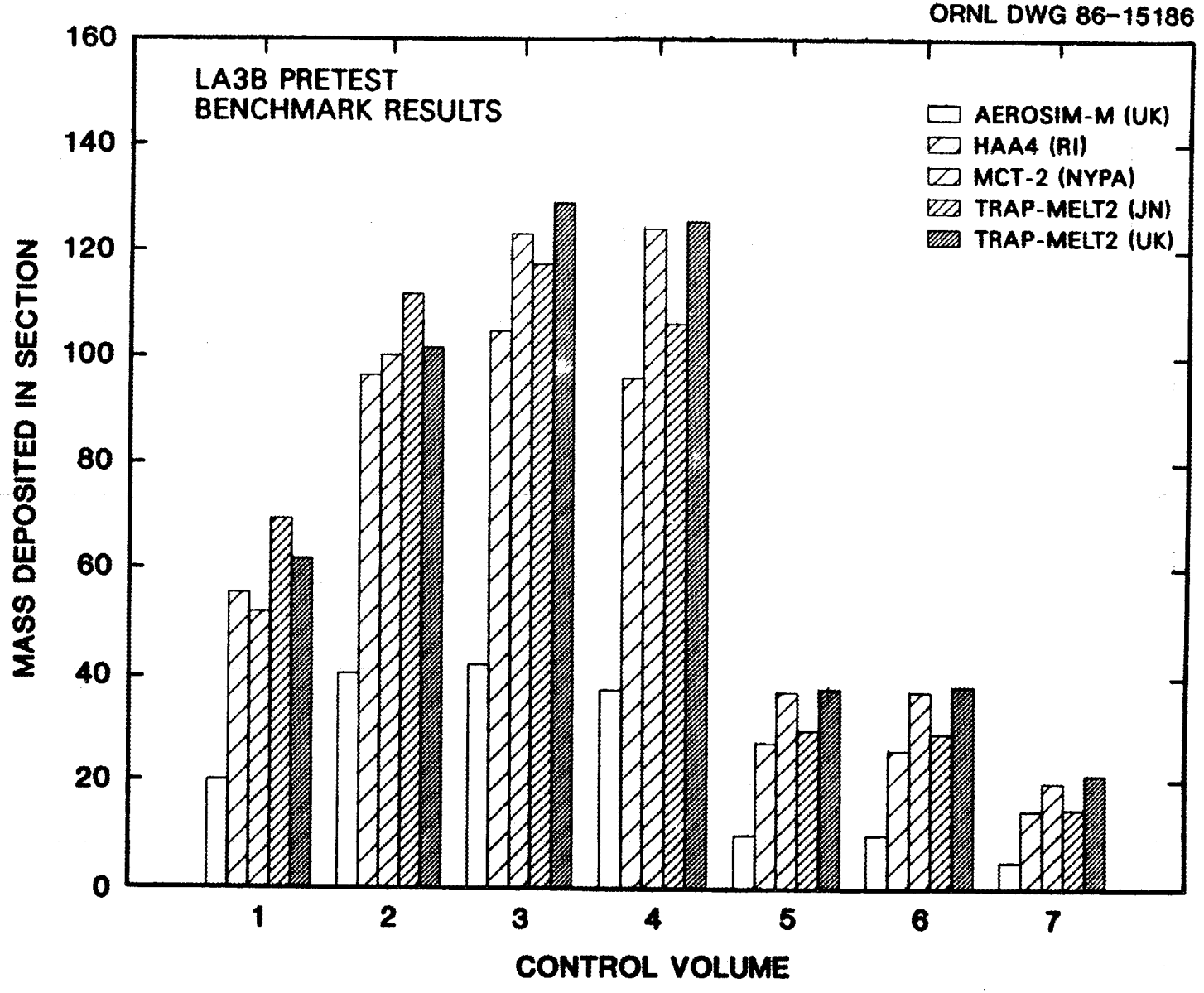

Fig. 18. LA3B benchmark pretest results: total aerosol deposited in each pipe control volume, at t = 3600 s.

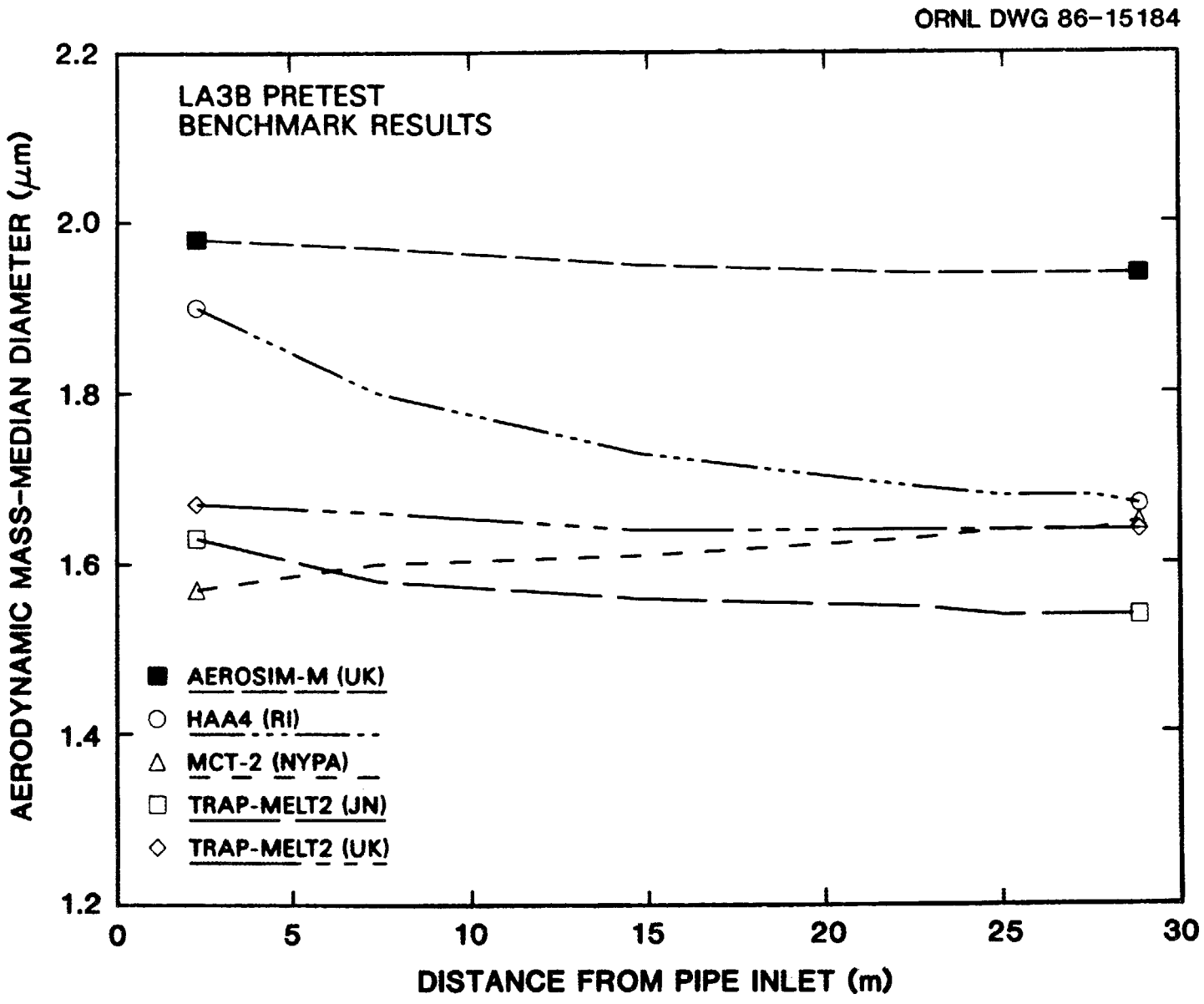

Fig. 19. LA3B benchmark pretest results: aerodynamic mass-median diameter vs distance from pipe inlet, at t = 3600 s.

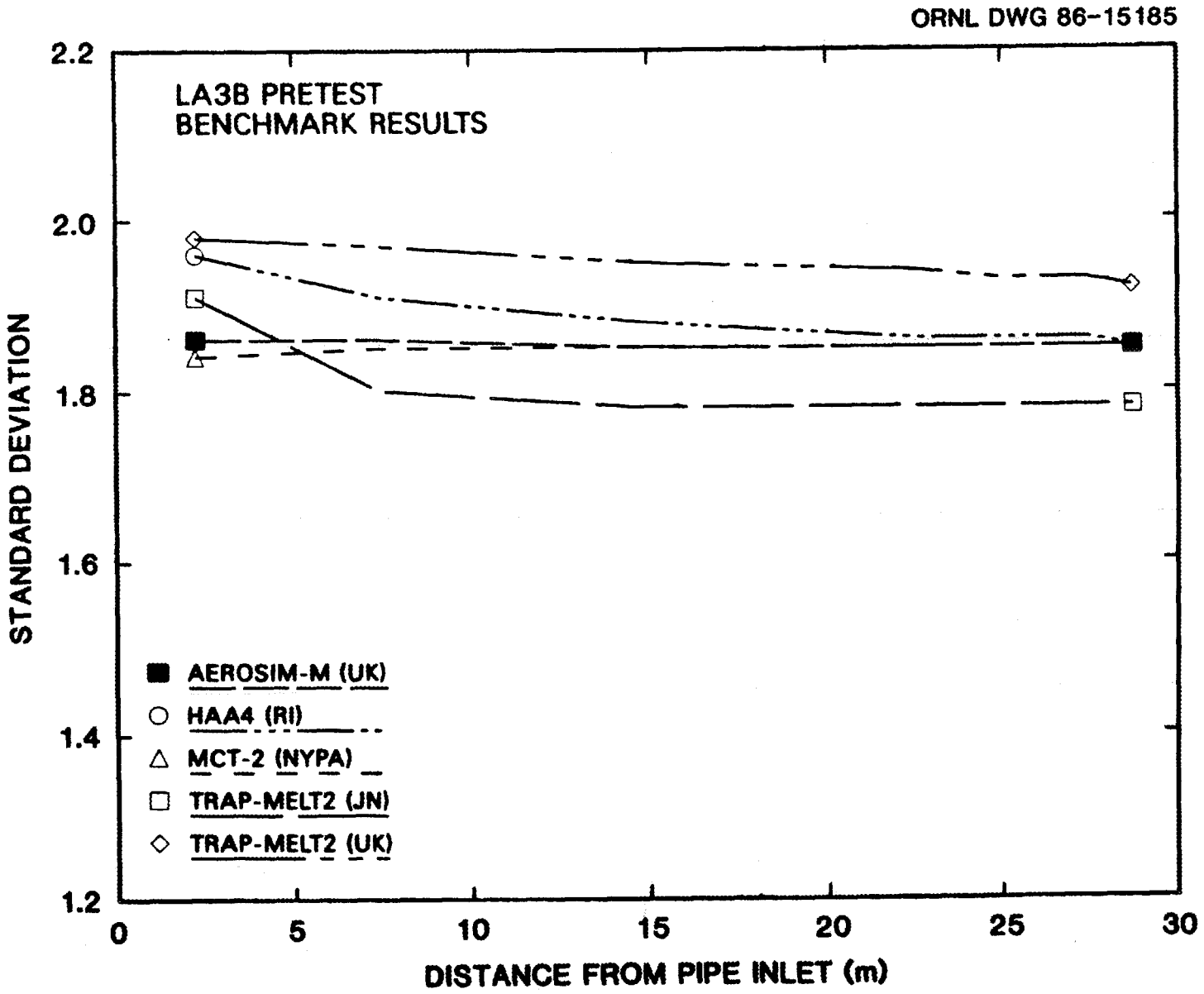

Fig. 20. LA3B benchmark pretest results: geometric standard deviation vs distance from pipe inlet, at t = 3600 s.

Table 13. Comparison of selected parameters from LA3B benchmark pretest calculations

Code	Range of calculated carrier-gas density (kg/m^3)	Range of calculated carrier-gas viscosity (kg/m-s)	Range of calculated carrier-gas flow velocity (m/s)	Range of calculated turbulent-deposition velocity (cm/s)
AEROSIM-M (UK)	0.57	2.4E-5	17.4	a
HAA4 (RI)	a	a	a	0.17-0.07
MCT-2 (NYPA)	0.51-0.56	2.4-2.2E-5	20.1-18.3	0.18-0.10
TRAP-MELT2 (JN)	a	a	a	0.37-0.12
TRAP-MELT2 (UK)	0.51-0.60	2.5-2.1E-5	20.1-17.1	0.19-0.10

[a]Data not provided for this parameter.

Table 14. Calculated deposition, by mechanism, for LA3B pretest benchmark calculation

Code	Calculated turbulent deposition (g)	Calculated deposition by thermophoresis (g)	Calculated deposition by settling (g)
AEROSIM-M	166	0	0
HAA4 (RI)	334	68	20
MCT-2 (NYPA)	417	58	19
TRAP-MELT2 (JN)	299	5	176
TRAP-MELT2 (UK)	399	48	70

data than did AEROSIM-M [see Sect. 2, Eqs. (6) and (8)], calculated similar deposition to that calculated by investigators using TRAP-MELT. The difference in the AEROSIM-M and HAA4 deposition results cannot presently be explained.

4. The AMMD results are shown in Fig. 19. Except for the MCT-2 calculation, all codes predicted that the AMMD decreased with distance from the pipe inlet. We cannot explain the calculated MCT-2 behavior. The TRAP-MELT AMMD values were again significantly less than those calculated by AEROSIM because of the TRAP-MELT code error in calculating AMMD, as discussed in Sect. 4. In the HAA4 calculation, the AMMD decreased more rapidly than for the others. Since the HAA4 calculation ignored aerosol agglomeration, this suggests that agglomeration in the other calculations caused the size distribution to remain nearly uniform; it also suggests that ignoring agglomeration may not be a good assumption for flow residence times that are greater than those expected in test LA3B.

5. Except for MCT-2, all calculations predicted that the airborne aerosol standard deviation decreased with distance from the pipe inlet; MCT-2 predicted a slight increase in σ_g.

6. SUMMARY AND CONCLUSIONS

A series of pretest calculations was performed to model the aerosol behavior expected in the LA3 test series (LA3A, LA3B, and LA3C). These tests were designed to investigate aerosol transport through a 0.063-m-diam, 28.8-m-long test pipe for simulated "containment bypass" accident sequence conditions. The major variables in the experiments were the gas flow velocity and the MnO/CsOH aerosol mass ratio input to the pipe. The major findings from this investigation are summarized as follows:

1. Aerosol deposition in the LA3 series, as it was in test LA1, was expected to occur largely by turbulent-inertial deposition. Section 3 of the report presented a comparison of calculated turbulent-deposition velocity vs particle size using five turbulent

deposition models;[4-7,9] flow conditions from tests LA1 and LA3 were used as a basis for the calculations. The main conclusions from this comparison were that (1) the Friedlander-Johnstone model appears not to correctly model experimental results for $\tau^+ > 33.3$; (2) the differences between the Liu-Agarwal and Battelle-Columbus test results, for τ^+ values $<\sim 10$, are not understood; (3) the Wood model results show that surface roughness can significantly influence turbulent deposition; and (4) none of the deposition-velocity measurements on which the various correlations and models are based were performed for high enough flow Reynolds numbers to simulate those produced in the LACE LA1 and LA3A experiments.

2. Results from the initial series of LA3 pretest calculations were presented in Sect. 4. The results showed that differences in calculated aerosol deposition were greater for the LA3B and LA3C test conditions (i.e., the tests performed at the lower flow velocity). Significant differences in the LA3B and LA3C TRAP-MELT (including MCT) calculations were observed; however, these were largely due to a code input error in the TRAP-MELT2 (UK) calculations. The AEROSIM-M calculation predicted the lowest amount of aerosol deposition for LA3B and LA3C conditions; the difference in AEROSIM-M and TRAP-MELT results may be explainable by differences in the turbulent-deposition correlations used in these codes.

3. Table 11 illustrated the calculated aerosol deposition due to turbulence, settling, and thermophoresis for the LA3 test conditions. The code predictions show that deposition by settling and thermophoresis may be significant for LA3B and LA3C test conditions. Errors in the TRAP-MELT2 (JN) values for settling areas caused this code to overcalculate settling by about a factor of 3.

4. Data from the LA3B benchmark calculations, in which all code analysts used the same pipe nodalization, were presented in Sect. 5. Deposition results from the three TRAP-MELT calculations were quite similar, largely because the earlier error in the TRAP-MELT2 (UK) calculation was corrected.

5. A modified version of the HAA4 code, a log-normal containment code, was used for the LA3B benchmark exercise. This version could, with the simplification that no aerosol agglomeration occurred as the aerosol flowed through the pipe, calculate the lengthwise variation of aerosol deposition. For the LA3B calculation, HAA4 calculated similar deposition to that calculated with TRAP-MELT but calculated greater deposition (by about a factor of 2) than that calculated by AEROSIM-M. We would have expected that HAA4 and AEROSIM-M would calculate similar deposition since the turbulent-deposition velocity correlations used in these codes are both based on the Liu-Agarwal experimental data. Finally, comparison of HAA4 and other code results for the change in AMMD with distance from the pipe inlet suggests that ignoring agglomeration in HAA4 may not be a good assumption for situations where pipe-flow residence times are greater than expected in the LA3B test.

6. Finally, we believe that the code users improved in their ability to perform valid pipe aerosol-deposition calculations by their participation in this exercise.

7. ACKNOWLEDGMENTS

We would like to thank the code analysts who participated in this study for their efforts and cooperation.

8. REFERENCES

1. D. R. Dickinson, Test Plan, LWR Aerosol Containment Experiment (LACE) Test LA3, Containment Bypass Conditions, Westinghouse Hanford Company, Mar. 17, 1986.

2. A. L. Wright, "Instructions for LA3 Pretest Aerosol Calculations," letter to LACE program participants, Oak Ridge National Laboratory, Apr. 16, 1986.

3. A. L. Wright, "Instructions for LA3B 'Benchmark' Pretest Calculation," letter to LACE program participants, Oak Ridge National Laboratory, July 23, 1986.

4. S. K. Friedlander and H. F. Johnstone, "Deposition of Suspended Particles from Turbulent Gas Streams," Ind. Eng. Chem. 49, 1151 (1957).

5. J. A. Gieseke, K. W. Lee, and M. A. Goldenberg, Measurement of Aerosol Deposition Rates in Turbulent Flows, NUREG/CR-1264, BMI-2041, Battelle-Columbus Laboratories, January 1980.

6. B. Y. H. Liu and J. K. Agarwal, "Experimental Observation of Aerosol Deposition in Turbulent Flow," J. Aerosol Sci. 5, 145 (1974).

7. J. M. Otter and E. U. Vaughan, HAA4 Code Description and User Manual, AI-DOE-13528, Rockwell International, December 1986.

8. A. L. Wright and P. C. Arwood, Summary of Posttest Aerosol Code Results for LWR Aerosol Containment Experiment (LACE) LA1, draft report issued to LACE participants, November 1986.

9. N. B. Wood, "A Simple Method for the Calculation of Turbulent Deposition to Smooth and Rough Surfaces," J. Aerosol Sci. 3, 275–90, (1981).

10. M. R. Kuhlman, V. Kogan, and P. M. Schumacher, TRAP-MELT2 Code: Development and Improvement of Transport Modeling, NUREG/CR-4677, BMI-2141, Battelle-Columbus Laboratories, July 1986.

11. J. H. Wilson and P. C. Arwood, Summary of Pretest Aerosol Code Results for LWR Aerosol Containment Experiment (LACE) LA2, LACE TR-004 (to be published).

LACE TR-023
ORNL/M-352

INTERIM DISTRIBUTION

1-3. P. C. Arwood
4. J. M. Asher
5. J. R. Hightower, Jr.
6. E. K. Johnson
7. T. S. Kress
8. R. A. Lorenz
9. A. P. Malinauskas
10. J. R. Merriman
11. M. G. Stewart
12. J. H. Wilson
13-15. A. L. Wright
16. R. G. Wymer
17-18. Technical Information Center, Department of Energy, P.O. Box 62, Oak Ridge, TN 37831
19. Office of Assistant Manager, Energy Research and Development, DOE-ORO, Oak Ridge, TN 37831
20. Laboratory Records - RC
21. ORNL Patent Section
22. Central Research Library
23. Document Reference Section